



**APPENDICES**

ลิขสิทธิ์มหาวิทยาลัยเชียงใหม่

Copyright© by Chiang Mai University

All rights reserved

## APPENDIX A

### 5.1 Strontium carbonate ( $\text{SrCO}_3$ ) and Barium carbonate ( $\text{BaCO}_3$ )

Strontium carbonate ( $\text{SrCO}_3$ ) and barium carbonate ( $\text{BaCO}_3$ ) are very important materials for a number of industries.  $\text{SrCO}_3$  is used as a constituent of ferrite magnets for small direct current motors, an additive in the production of glass for color television tubes, modern electric industries, and for the production of iridescent and special glasses, pigments, driers, paints, pyrotechnics, strontium metals and other strontium compounds [70–71].  $\text{BaCO}_3$  has also attracted attention due to its close relationship with aragonite and many important applications in ceramic and optical glass industries. It is also a highly utilized precursor for the synthesis of barium ferrites and ferroelectric materials [74,75].

In recent years, ultrasonic radiation (20 kHz–10MHz) [74,76] has been used to prepare nanoparticles [74,76]. The chemical effects of the ultrasound arise from acoustic cavitation—formation, growth, and implosive collapse of bubbles in liquids. There are two regions of sonochemical reactivity, the inside zone of the collapsing bubble and the interface between bubbles and the liquid. The cavitation may generate very high temperature over 5000 K and pressure over 20 MPa, which enable many chemical reactions to occur. In short, during the process, the implosive collapse of bubbles generates localized hot spots through adiabatic compression or shockwave formation within the gas phase of the collapsing bubbles. These extreme conditions attained during bubble collapse have been exploited to prepare various materials with different morphologies [76,77].

In our work,  $\text{SrCO}_3$  and  $\text{BaCO}_3$  nanoparticles were synthesized by sonochemical method using strontium nitrate or barium nitrate and sodium carbonate as starting materials at  $80\text{ }^\circ\text{C}$  for 1–5 h.

### 5.1.1 Physical properties

#### 5.1.1.1 Crystal structure of $\text{SrCO}_3$ and $\text{BaCO}_3$

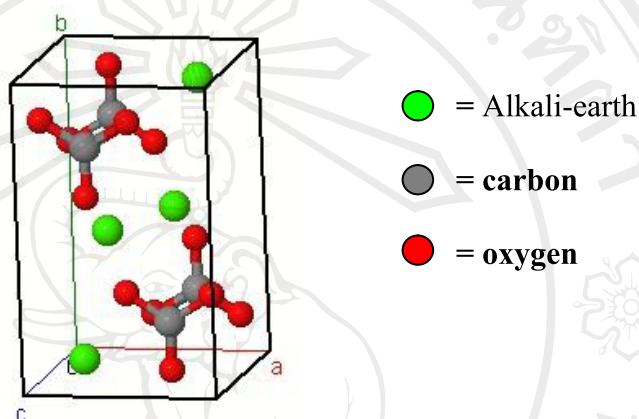


Figure 5.1 Crystal structures of Alkali-earth (and other  $\text{M}^{2+}$ ) carbonates

#### 5.1.1.2 Chemical properties

Strontium carbonate is a white, odorless, tasteless powder. Its chemical makeup is: C 8.14% O 32.51% Sr 59.35%. Being a carbonate, it is a weak base and therefore is reactive with acids. It is otherwise stable and safe to work with. It is practically insoluble in water (1 part in 100,000). The solubility is increased significantly if the water is saturated with carbon dioxide, to 1 part in 1,000. It is soluble in dilute acids.

Barium carbonate is a white, odorless, tasteless powder. Its chemical makeup is: C 6.08% O 24.32% Ba 69.60%. Being a carbonate, it is a weak base and therefore is reactive with acids. It is otherwise stable and safe to work with. It is practically insoluble in water (0.0024 g/100 mL ( $20\text{ }^\circ\text{C}$ )). The solubility is increased significantly if the water is saturated with carbon dioxide. It is soluble in dilute acids.

Barium carbonate reacts with many acids to soluble barium salts, for example barium chloride:



However the reaction with sulfuric acid is poor, because barium sulfate is highly insoluble

### 5.1.2 Applications

Strontium carbonate ( $\text{SrCO}_3$ ) and barium carbonate ( $\text{BaCO}_3$ ) are very important materials for a number of industries.  $\text{SrCO}_3$  is used as a constituent of ferrite magnets for small direct current motors, an additive in the production of glass for color television tubes, modern electric industries, and for the production of iridescent and special glasses, pigments, driers, paints, pyrotechnics, strontium metals and other strontium compounds [70-73].  $\text{BaCO}_3$  has also attracted attention due to its close relationship with aragonite and many important applications in ceramic and optical glass industries. It is also a highly utilized precursor for the synthesis of barium ferrites and ferroelectric materials [74,75].

### 5.1.3 Literature Review

Ma and Zhu [77] have synthesized by a microwave heating time plays an important role in the size and morphology of  $\text{SrCO}_3$ . The products were characterized by X-ray powder diffraction (XRD), scanning electron microscopy (SEM), transmission electron microscopy (TEM) and selected-area electron diffraction (SAED). So, it was expected to preparation of nanostructure of other kinds of carbonate.

Li *et al.* [70] have synthesized flower-like SrCO<sub>3</sub> nanostructures by a convenient hydrothermal process. X-ray powder diffraction (XRD) pattern reveals that the flower-like SrCO<sub>3</sub> nanostructures are of orthorhombic phase. This method was more selected area electron diffraction (SAED) and high resolution transmission electron microscopy (HRTEM). They also discussed the formation mechanism of the SrCO<sub>3</sub> nanostructures has been preliminary presented.

Yu *et al.* [78] have prepared SrCO<sub>3</sub> by a simple precipitation reaction with strontium nitrate in the absence and presence of poly-(styrene-alt-maleic acid) (PSMA). The result showed that SrCO<sub>3</sub> particles with various shapes, bundles, dumbbells, irregular aggregates and spheres could be obtained by varying the concentration of PSMA. In addition, the shape evolution of the as-prepared SrCO<sub>3</sub> particles.

Shi and Du [79] have prepared SrCO<sub>3</sub> hexahedral by a simple solvothermal route at 120 °C using glycerin as the solvent to control morphology. X-ray powder diffraction (XRD) and field-emission scanning electron microscopy (FE-SEM) were used characterized such hexahedral ellipsoids. They also discussed the growth mechanism of the SrCO<sub>3</sub> hexahedral ellipsoids has been preliminary presented.

Shi and Du [80] have prepared fusiform hexagonal prism SrCO<sub>3</sub> microrods by a simple solvothermal route at 120 °C and characterized by X-ray powder diffraction (XRD), field-emission scanning electron microscopy (FE-SEM) and Fourier transform infrared (FT-IR) spectroscopy. It was found that ethylene glycol (EG) played an important role in the formation of such SrCO<sub>3</sub> microrods. So the effects of other solvents on the products, 1,2 propanediol and glycerin were also investigated.

Alavi and Morsali [74] have synthesized BaCO<sub>3</sub> nanostructures by the reaction of Ba(CH<sub>3</sub>COO)<sub>2</sub> and sodium hydroxide or tetramethylammonium hydroxide (TMAH) by a sonochemical method. Reaction conditions, such as the concentration of the Ba<sup>2+</sup> ion, aging time and power of the ultrasonic device played important roles in the size, morphology and growth process of the final products. The BaCO<sub>3</sub> nanostructures were characterized by scanning electron microscopy (SEM), X-ray powder diffraction (XRD), and the Infrared spectroscopy (IR).

Li *et al.* [75] have successfully synthesized BaCO<sub>3</sub> in CTAB/cyclohexane/H<sub>2</sub>O and NP10/ cyclohexane/H<sub>2</sub>O microemulsion. The samples were characterized by transmission electron microscopy (TEM), X-ray diffraction (XRD) and infrared spectroscopy (IR). The possible mechanisms for the formation of BaCO<sub>3</sub> samples in series of microemulsion systems were discussed. Various comparison experiments show that several experimental parameters, such as the concentration of surfactant and reactant, and solvent hydrothermal treatment play important roles in the morphological control of BaCO<sub>3</sub> nanostructures.

Ma *et al.* [81] have synthesized BaCO<sub>3</sub> nanostructures by using Ba(NO<sub>3</sub>)<sub>2</sub> and (NH<sub>4</sub>)<sub>2</sub>CO<sub>3</sub> in the water/ethylene glycol (EG) mixed solvents by oil bath heating at 80 °C for 30 min. The molar ratio of water to EG had an effect on the morphology of BaCO<sub>3</sub>. The products were characterized by X-ray powder diffraction (XRD), scanning electron microscopy (SEM), transmission electron microscopy (TEM), and high-resolution transmission electron microscopy (HRTEM).

Ma *et al.* [82] have synthesized BaCO<sub>3</sub> by using Ba(NO<sub>3</sub>)<sub>2</sub> and (NH<sub>4</sub>)<sub>2</sub>CO<sub>3</sub> (or Na<sub>2</sub>CO<sub>3</sub> or NaHCO<sub>3</sub>) in water at room temperature for 30 min. The CO<sub>3</sub><sup>2-</sup> source played an important role in the morphology of BaCO<sub>3</sub>. The influences of different



surfactants such as cetyltrimethyl ammonium bromide (CTAB), sodium dodecyl benzene sulfonate (SDBS), and triblock copolymer poly(ethylene glycol)-block-poly(propylene glycol)-block poly(ethylene glycol) (P123) on the morphology of  $\text{BaCO}_3$  were also investigated. A rational mechanism of rod-like shape assembled from nanoparticles was proposed. The products were characterized by X-ray powder diffraction (XRD), scanning electron microscopy (SEM), transmission electron microscopy (TEM), and selected area electron diffraction (SAED).

Lv *et al.* [83] have successfully synthesized  $\text{BaCO}_3$  by a simple PVP-assisted method. Reaction conditions, such as pH value, the ratio of EDTA/ $\text{Ba}^{2+}$  and the concentration of the  $\text{Ba}^{2+}$  ions are found to play important roles in determining the morphologies and growth process of the final products. X-ray diffraction (XRD), transmission electron microscope (TEM), selected area electron diffraction (SAED) and the infrared (IR) spectrum of the sample are used to characterize the obtained products.

Bostow [84] have studied the Mg, Sr and Ba sites in  $\text{MgCO}_3$ ,  $\text{SrCO}_3$  and  $\text{BaCO}_3$  by nuclear magnetic resonance. The result showed that for the  $V_{zz}$  at the Ca site in the calcite and aragonite forms of  $\text{CaCO}_3$ , have been compared with ab initio electronic structure calculations using the density functional based code for crystalline solids, WIEN 97. So, the agreement between the theoretical and experimental values of  $V_{zz}$  is found to be within 10%.

Vov *et al.* [85] have studied on the decompositions of  $\text{CaCO}_3$ ,  $\text{SrCO}_3$  and  $\text{BaCO}_3$  in the presence of  $\text{CO}_2$  and some data reported in the literature were used for the determination of the  $E$  parameter of the Arrhenius equation by the third-law method. The values obtained (495, 569 and  $605 \text{ kJ mol}^{-1}$ ) are twice as much

compared with the values of the  $E$  parameter obtained for these carbonates earlier in the absence of  $\text{CO}_2$ . This fact together with the invariance of the  $E$  parameter with partial pressure of  $\text{CO}_2$  ( $P_{\text{CO}_2}$ ) and a hyperbolic dependence of the rate of decomposition on  $P_{\text{CO}_2}$  is in excellent agreement with the theoretical predictions deduced from the mechanism of decomposition that includes the primary stage of dissociative evaporation of reactant.

Thongtem *et al.* [86] have synthesized  $\text{BaCO}_3$  and  $\text{SrCO}_3$  nanoparticles by using  $\text{Sr}(\text{NO}_3)_2$  or  $\text{Ba}(\text{NO}_3)_2$  and  $\text{Na}_2\text{CO}_3$  as starting materials in ethylene glycol by ultrasonic irradiation at  $80^\circ\text{C}$  for 1–5 h. Their phases, vibration modes and morphologies were characterized using X-ray powder diffraction (XRD), Fourier transform infrared (FTIR) spectroscopy, selected area electron diffraction (SAED) and transmission electron microscopy (TEM). These products were found to be orthorhombic  $\text{SrCO}_3$  and  $\text{BaCO}_3$  nanoparticles with 20–50 nm and 40–100 nm ranges, respectively. Asymmetric stretching, symmetric stretching, and out of plane and in plane bending vibrations of  $\text{CO}_3^{2-}$  complexes were also detected.



## EXPERIMENTAL PROCEDURE

### 5.2 Chemical reagents and equipments

#### 5.2.1 Chemical reagents

- 1) Ethylene glycol, EG, Mr = 62.070, >98%, Carlo Erba
- 2) Strontium nitrate,  $\text{Sr}(\text{NO}_3)_2$ , MW = 211.65, >98%, Reidel
- 3) Barium nitrate,  $\text{Ba}(\text{NO}_3)_2$ , MW = 261.35, >98%, Fluka
- 4) Sodium carbonate,  $\text{Na}_2\text{CO}_3$ , MW = 105.99, >98%, Fluka
- 5) Deionized water
- 6) Ethanol,  $\text{C}_2\text{H}_5\text{OH}$ , 95%, Merck
- 7) Absolute ethanol,  $\text{C}_2\text{H}_5\text{OH}$ , 99.0-100.0% AR, Merck

#### 5.2.2 Equipments

- 1) Hotplate and magnetic stirrer, model 502P-2, PMC Industries, Inc., San Diego, U.S.A.
- 2) Analytical balance, Model BP-210S, Satorius AG. Goettingen, Germany
- 3) Oven, Model UE-400, Memmert, Germany
- 4) Ultrasonic bath, Bandelin Sonorex, Germany
- 5) X-ray Diffractometer, model D500/501, Siemens, Germany
- 6) Fourier Transform Infrared Spectrophotometer, FT-IR 510 Nicolet, U.S.A.
- 7) Raman spectroscopy, model T64000 JY, Horiba Jobin Yvon, France
- 8) Perkin Elmer Luminescence spectrometer, model LS50B
- 9) Scanning Electron Microscope, model JSM-6335, JEOL, Japan

10) Transmission Electron Microscope, model JEM-2010,

JEOL, Japan

11) Agate mortar

### 5.3 Synthesis of SrCO<sub>3</sub> and BaCO<sub>3</sub> using a sonochemical method

BaCO<sub>3</sub> and SrCO<sub>3</sub> nanocrystallines were synthesized by the reactions of 0.005 mol of Ba(NO<sub>3</sub>)<sub>2</sub> or Sr(NO<sub>3</sub>)<sub>2</sub> and 0.005 mol Na<sub>2</sub>CO<sub>3</sub> as starting materials in 50 ml ethylene glycol, without the use of any catalysts or calcination at high temperatures. The solutions were transferred into 125 ml flasks. Each was put in an ultrasonic bath (Bandelin SONOREXRK 102 H, 120/480W, 35 kHz, inner dimension: 22 cm long×13.5 cm wide×10 cm deep), and sonicated at 80 °C for 1 h, 3 h, and 5 h at a time. Calculated maximum intensity is 16, 162Wm<sup>-2</sup>. The final products were washed with water and ethanol, and dried at 70 °C for 12 h. The phases, vibration modes and morphologies of the products were characterized using X-ray diffraction (XRD) recorded on a D-500 Siemens X-ray diffractometer with Cu K<sub>α</sub> radiation and the diffraction angles of 2θ = 10-60° range, Bruker Tensor27 Fourier transform infrared (FTIR) spectrometer with KBr as a diluting agent operated in 400–4000 cm<sup>-1</sup> range, transmission electron microscope (TEM) carried out on a JEM-2010 JEOL TEM at 200 kV.

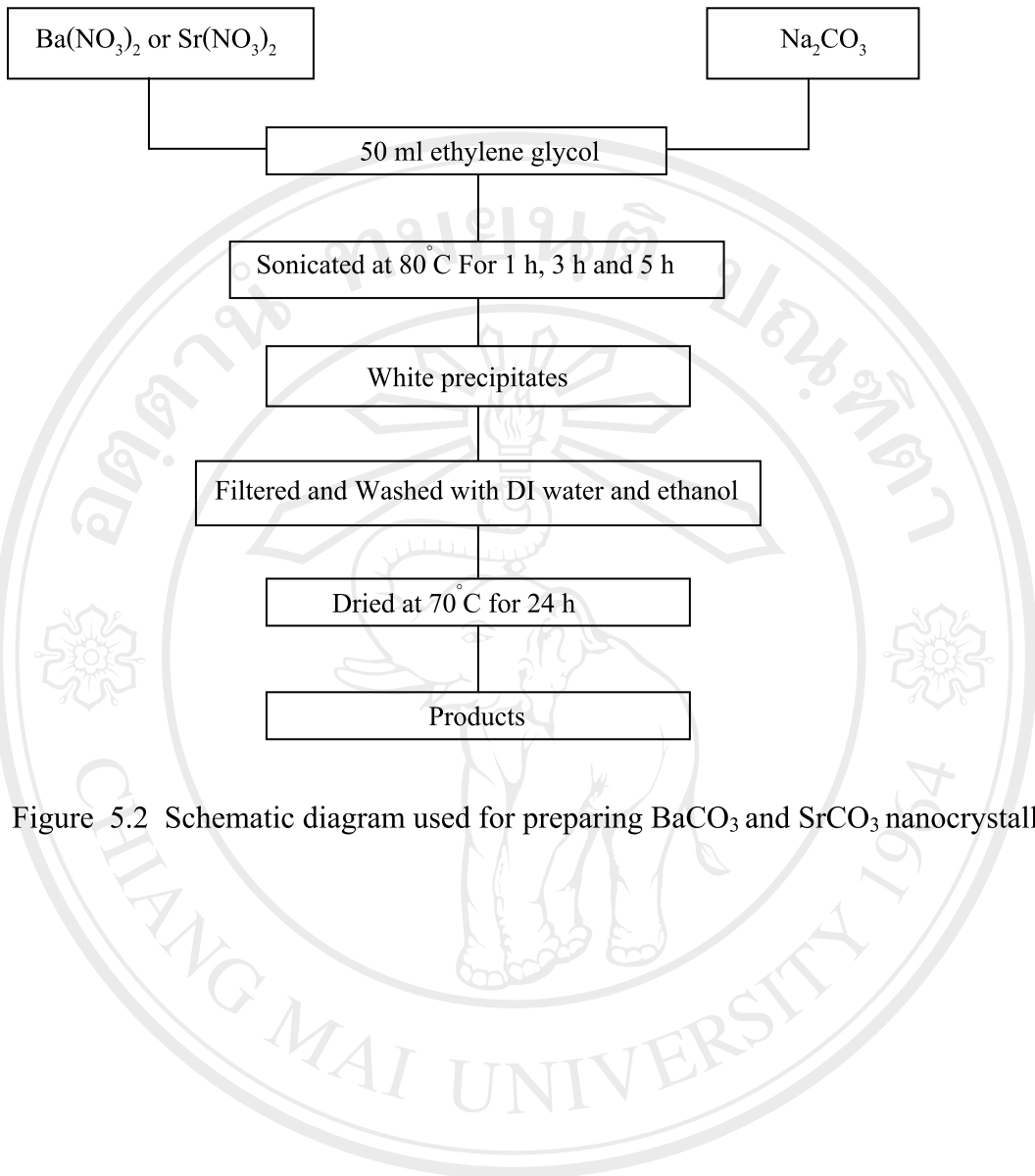


Figure 5.2 Schematic diagram used for preparing  $\text{BaCO}_3$  and  $\text{SrCO}_3$  nanocrystallines

#### 5.4 Result of SrCO<sub>3</sub> and BaCO<sub>3</sub> using a sonochemical method

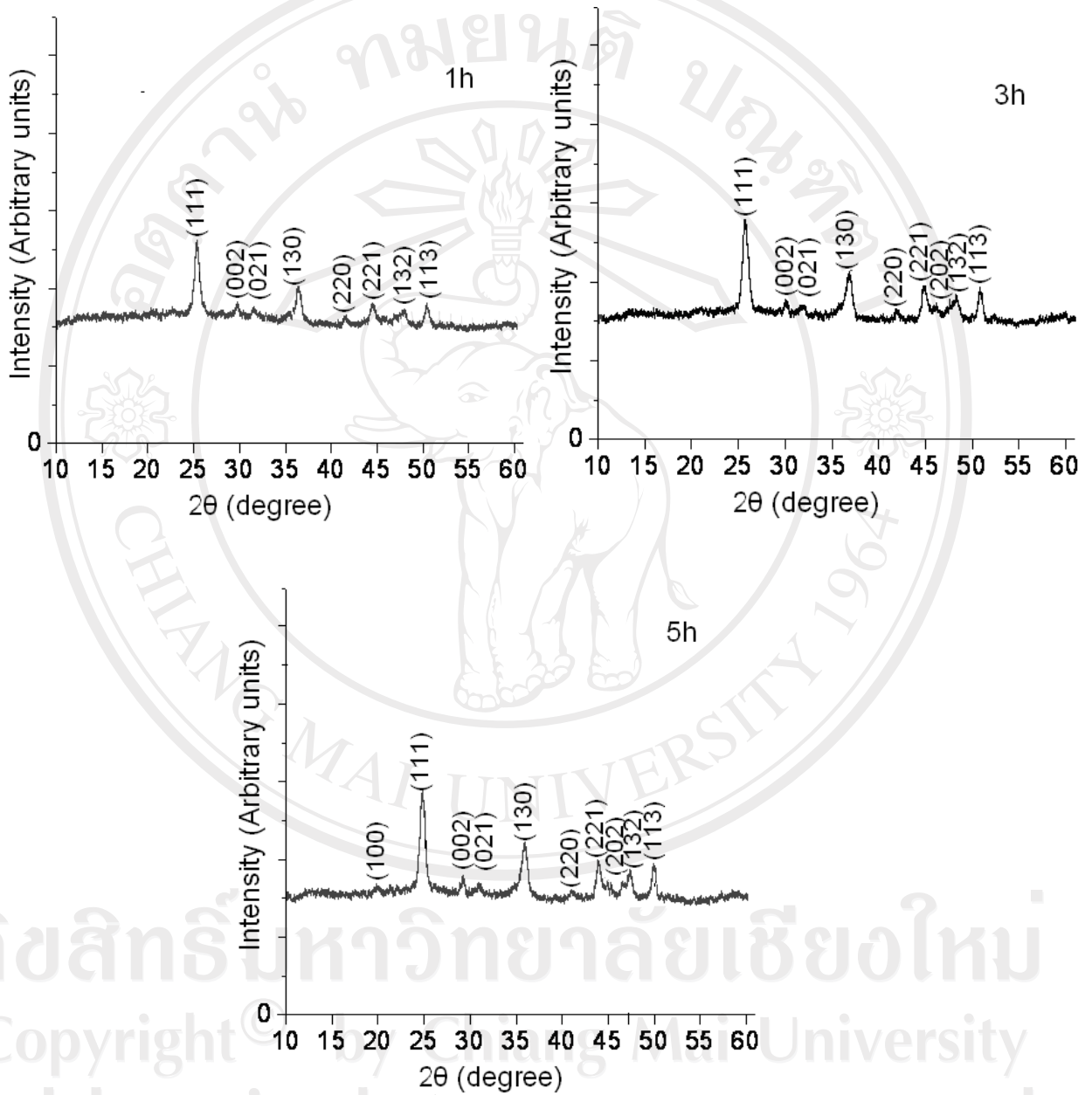


Figure 5.3 XRD patterns of SrCO<sub>3</sub> synthesized by the sonochemical method at 80 °C for different lengths of times using Sr(NO<sub>3</sub>)<sub>2</sub> and Na<sub>2</sub>CO<sub>3</sub> as material sources.

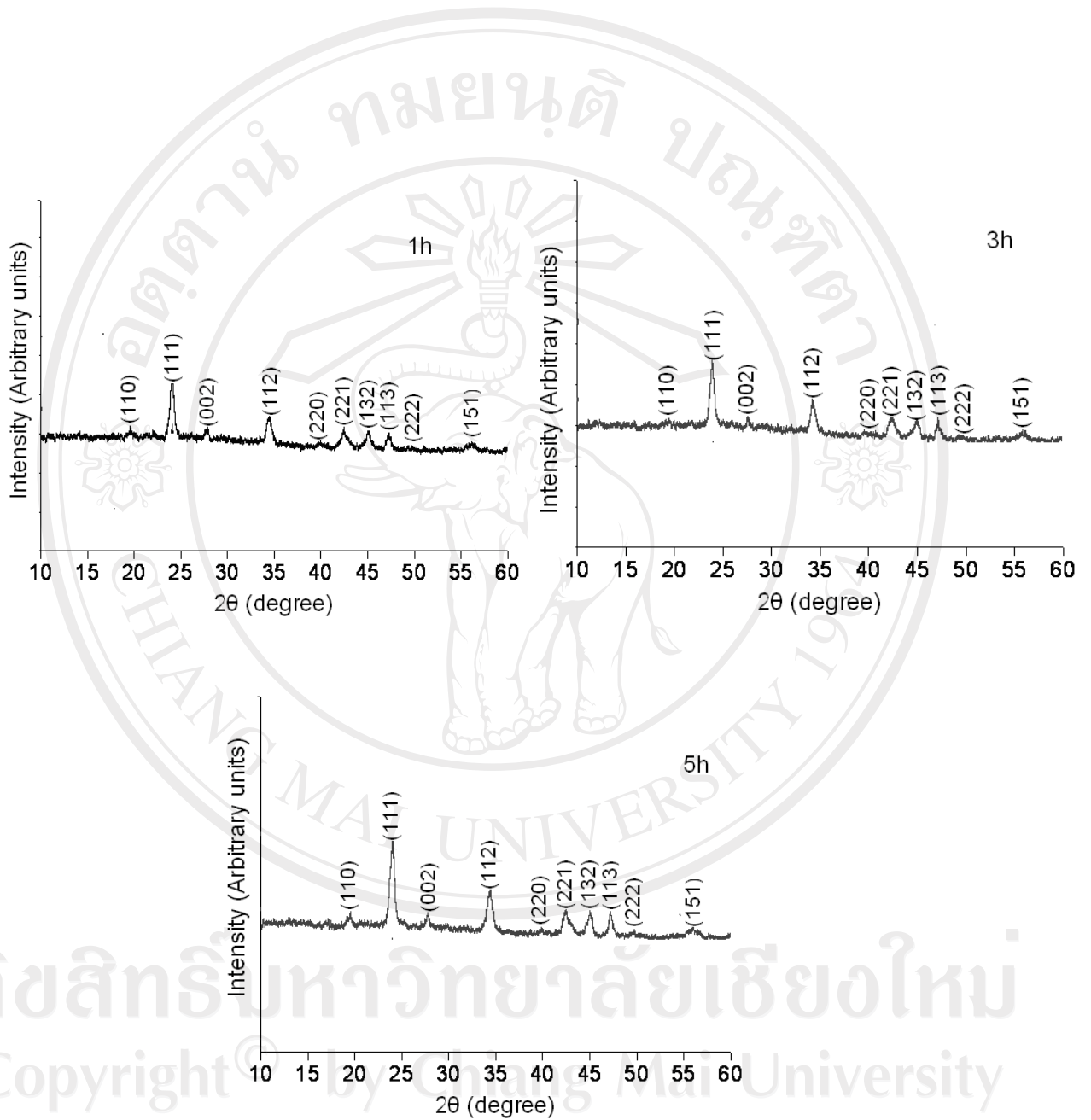


Figure 5.4 XRD patterns of BaCO<sub>3</sub> synthesized by the sonochemical method at 80 °C for different lengths of times using Ba(NO<sub>3</sub>)<sub>2</sub> and Na<sub>2</sub>CO<sub>3</sub> as material sources.

Typical XRD patterns of the as synthesized SrCO<sub>3</sub> and BaCO<sub>3</sub> nanocrystallines are shown in Figure 5.3-5.4. All diffraction peaks were identified to be orthorhombic SrCO<sub>3</sub>—compared to the JCPDS No. 05-0418 (a=5.1070 Å, b=8.4140 Å and c=6.0290 Å and α=β=γ=90°) and orthorhombic BaCO<sub>3</sub>—compared to the JCPDS No. 05-0378 (a=5.3140 Å, b=8.9040 Å and c=6.4300 Å and α=β=γ=90°) [87]. Slightly broadened diffraction peaks with 2θ (°) of 20.45, 25.35, 29.73, 31.62, 36.58, 41.73, 44.52, 46.90, 48.02 and 50.43 were readily indexed as the (110), (111), (002), (012), (130), (220), (221), (202), (132) and (113) planes for SrCO<sub>3</sub>; and 19.54, 23.99, 27.68, 29.71, 34.32, 39.62, 42.42, 44.28, 44.98, 55.70 and 56.15 as the (110), (111),(002), (012), (130), (220), (221), (202), (132), (241) and (151) planes for BaCO<sub>3</sub>, respectively. The increase in lattice parameters from SrCO<sub>3</sub> to BaCO<sub>3</sub> seems to relate with their ionic radii of these alkaline earth metals (Sr<sup>2+</sup>=0.125 nm and Ba<sup>2+</sup>=0.142 nm) [88]. The Scherrer formula [74] was used to determine the crystallite sizes of SrCO<sub>3</sub> and BaCO<sub>3</sub> as follows:

$$L = \frac{\lambda}{B \cos \theta} \quad (1)$$

where λ is the wavelength of Cu Kα radiation (0.154178 nm [70]), θ is the Bragg angle at the (111) peaks of the XRD patterns, L is the average crystallite sizes of SrCO<sub>3</sub> and BaCO<sub>3</sub>, k is the constant (0.89), and B is the full width at half maximum of the (111) peaks in radian. Calculated crystallite sizes of the products synthesized by the sonochemical method for 1 h, 3 h and 5 h are 8.74, 10.93 and 12.11 nm for SrCO<sub>3</sub>, and 14.72, 16.38 and 19.52 nm for BaCO<sub>3</sub>, respectively. These particle sizes were



enlarged with the length of reaction time. At same length of time, the particle sizes of  $\text{BaCO}_3$  are larger than those of  $\text{SrCO}_3$ , due to the increase in their ionic radii and atomic masses.

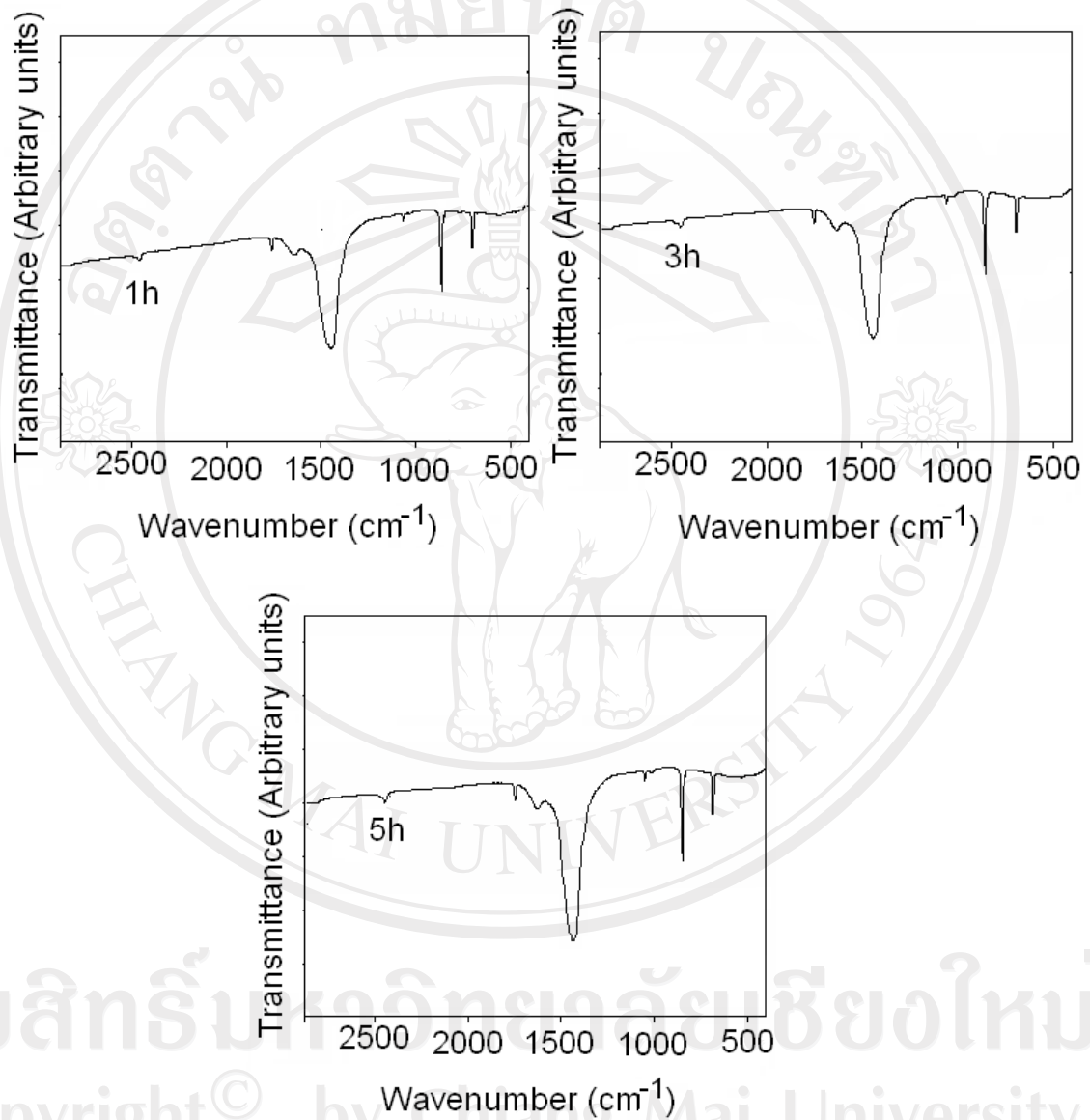


Figure 5.5 FITR spectra of  $\text{SrCO}_3$  synthesized by the sonochemical method at 80 °C for different lengths of times.

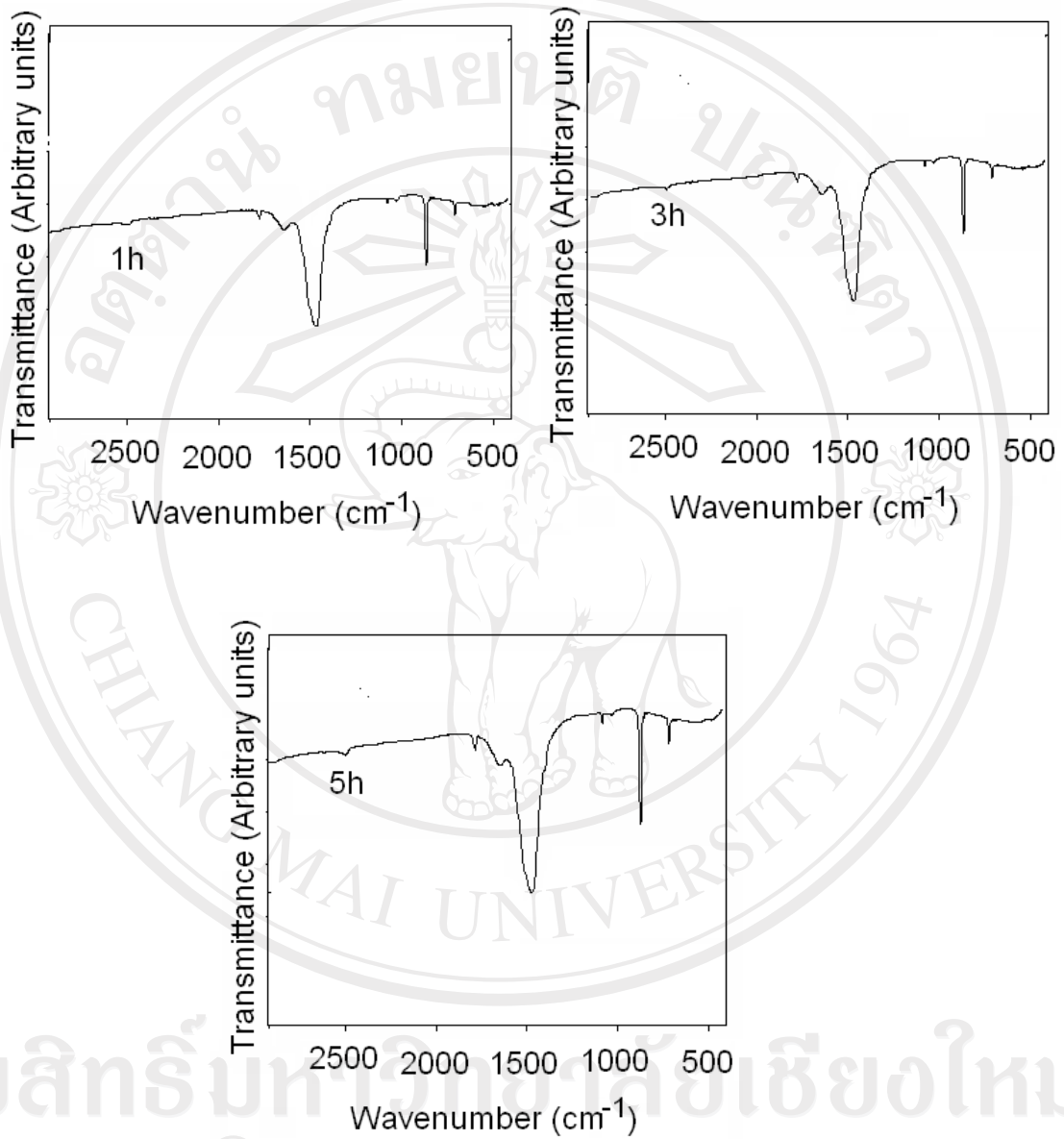


Figure 5.6 FTIR spectra of BaCO<sub>3</sub> synthesized by the sonochemical method at 80 °C for different lengths of times.

Figure 5.5-5.6 shows FTIR spectra of SrCO<sub>3</sub> and BaCO<sub>3</sub>, recorded in the 400–4000 cm<sup>-1</sup> wavenumbers. In general, the free planar CO<sub>3</sub><sup>2-</sup> complexes have D<sub>3h</sub> symmetry. The absorption bands were caused by the vibrations in CO<sub>3</sub><sup>2-</sup> at 400–1800 cm<sup>-1</sup>. The strong absorption bands, centered at about 1449 cm<sup>-1</sup> for SrCO<sub>3</sub> and 1447 cm<sup>-1</sup> for BaCO<sub>3</sub>, are connected with the asymmetric stretching vibrations. Strong narrow absorption bands at about 865 cm<sup>-1</sup> and 707 cm<sup>-1</sup> for SrCO<sub>3</sub>, and 862 cm<sup>-1</sup> and 696 cm<sup>-1</sup> for BaCO<sub>3</sub> are assigned to be out of plane bending vibrations and in plane bending vibrations, SrCO<sub>3</sub> and 1060 cm<sup>-1</sup> for BaCO<sub>3</sub>, due to the symmetric stretching vibrations, were also detected [73–75,89]. It is worth to note that these vibrations were shifted from the higher wave numbers for SrCO<sub>3</sub> to the lower ones for BaCO<sub>3</sub>, due to the covalent bonding of M<sup>2+</sup> cations (M=Sr and Ba) and O<sup>2-</sup> anions in the [CO<sub>3</sub>]<sup>2-</sup> complexes—the cause of changing the efficient masses of the oscillating atomic groups. In addition, O–H stretching and bending vibrations of residual water were respectively detected at 3466 and 1633 cm<sup>-1</sup> for SrCO<sub>3</sub>, and 3462 and 1640 cm<sup>-1</sup> for BaCO<sub>3</sub>.

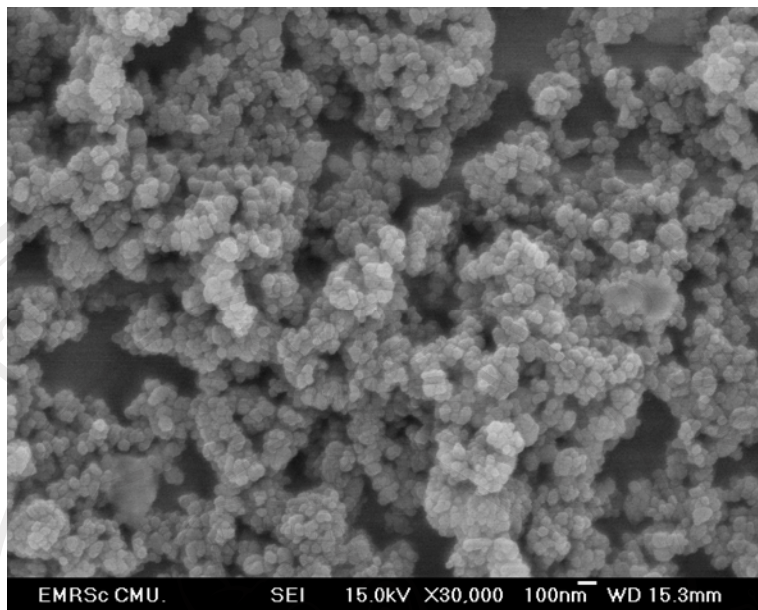


Figure 5.7 SEM image of SrCO<sub>3</sub> synthesized by sonochemical method at 80 °C for 1 h.

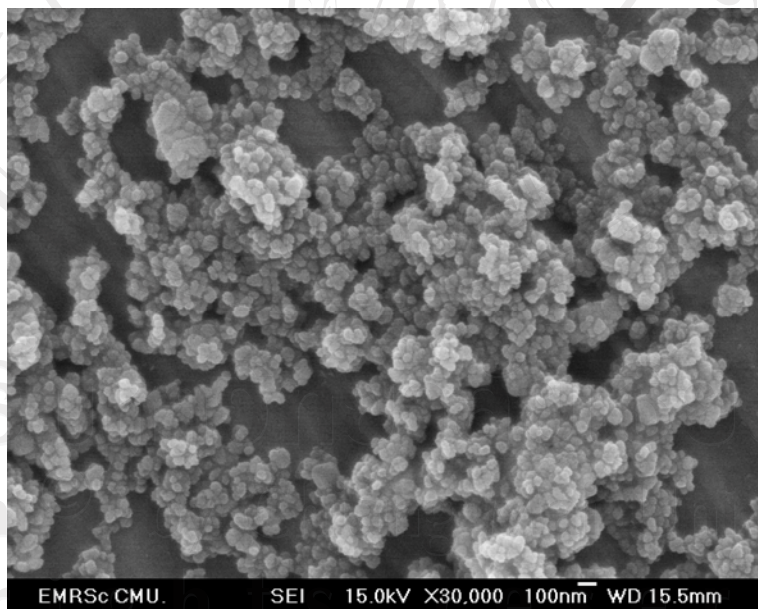


Figure 5.8 SEM image of SrCO<sub>3</sub> synthesized by sonochemical method at 80 °C for 3 h.

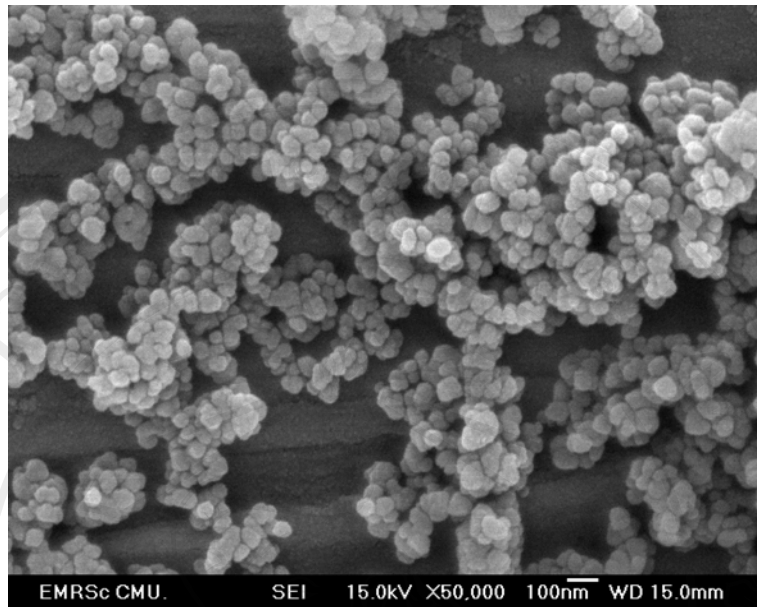


Figure 5.9 SEM image of SrCO<sub>3</sub> synthesized by sonochemical method at 80 °C for 5 h.

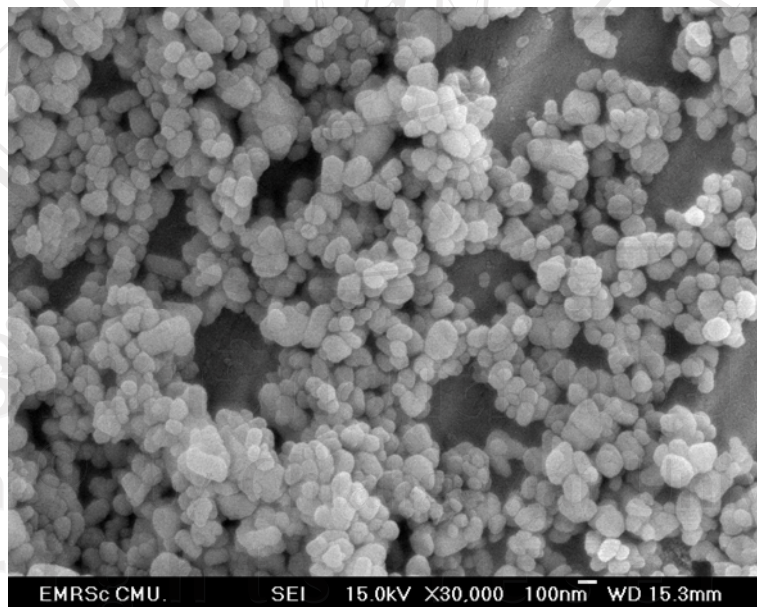


Figure 5.10 SEM image of BaCO<sub>3</sub> synthesized by sonochemical method at 80 °C for 1 h.



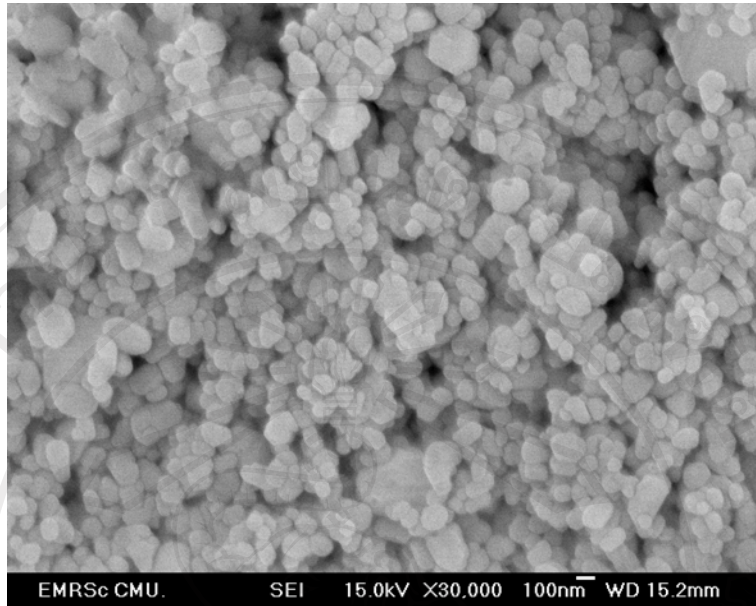


Figure 5.11 SEM image of BaCO<sub>3</sub> synthesized by sonochemical method at 80 °C for 3 h.

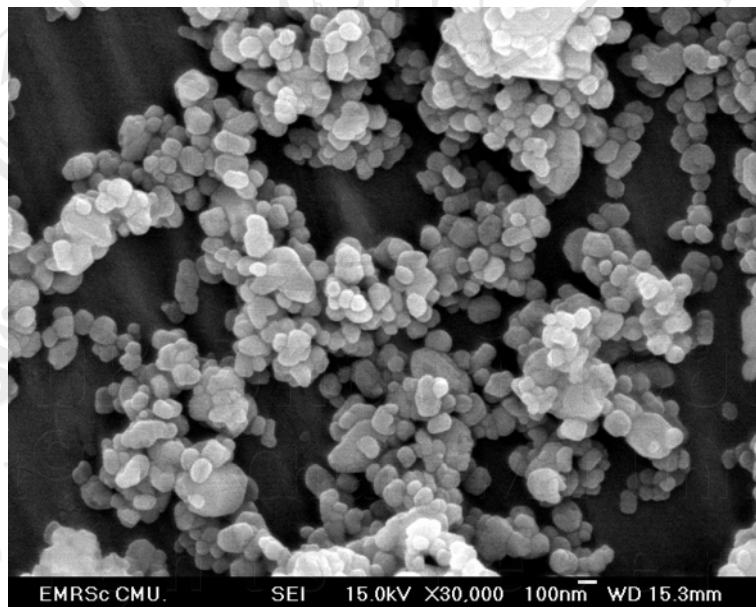


Figure 5.12 SEM image of BaCO<sub>3</sub> synthesized by sonochemical method at 80 °C for 5 h.



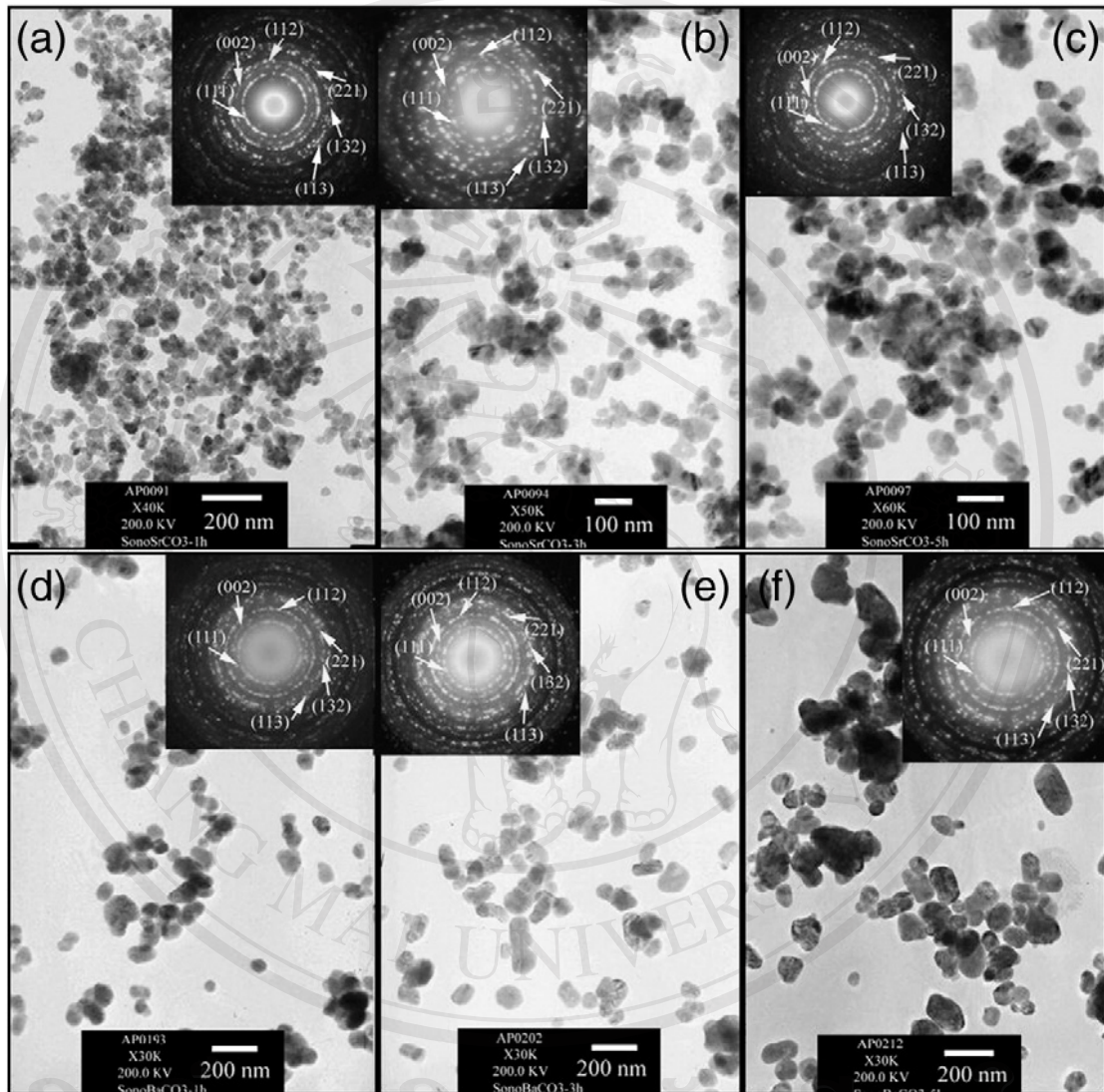


Figure 5.13 TEM images and SAED patterns of (a–c)  $\text{SrCO}_3$  and (d–f)  $\text{BaCO}_3$  synthesized by sonochemical method at  $80^\circ\text{C}$  for 1 h, 3 h and 5 h, respectively.

TEM images and SAED patterns of  $\text{SrCO}_3$  and  $\text{BaCO}_3$  are shown in Figure 5.13. TEM shows that the products were composed of dispersed round nanoparticles with the sizes of 20–50 nm for  $\text{SrCO}_3$  and 40–100 nm for  $\text{BaCO}_3$ . Their SAED patterns appear as diffuse and hollow concentric rings of bright spots, caused by the diffraction of transmitted electrons through the nanocrystals with different

orientations. Inter planar spaces were calculated using diameters of the diffraction rings [90], and compared with those of the JCPDS database [87]. They correspond to the (111), (002), (112), (221), (132) and (113) planes for both SrCO<sub>3</sub> and BaCO<sub>3</sub>. Their sizes were measured from 150 particles on TEM images. The products were synthesized in all sizes, ranging from the smallest to the largest with the average of 29.83±4.26 nm, 34.02±5.26 nm and 37.20±5.86 nm for SrCO<sub>3</sub>, and 55.20±9.60 nm, 65.00±10.04 nm and 89.56±16.10 nm for BaCO<sub>3</sub> by the 1 h, 3 h and 5 h ultrasonic irradiation, respectively.

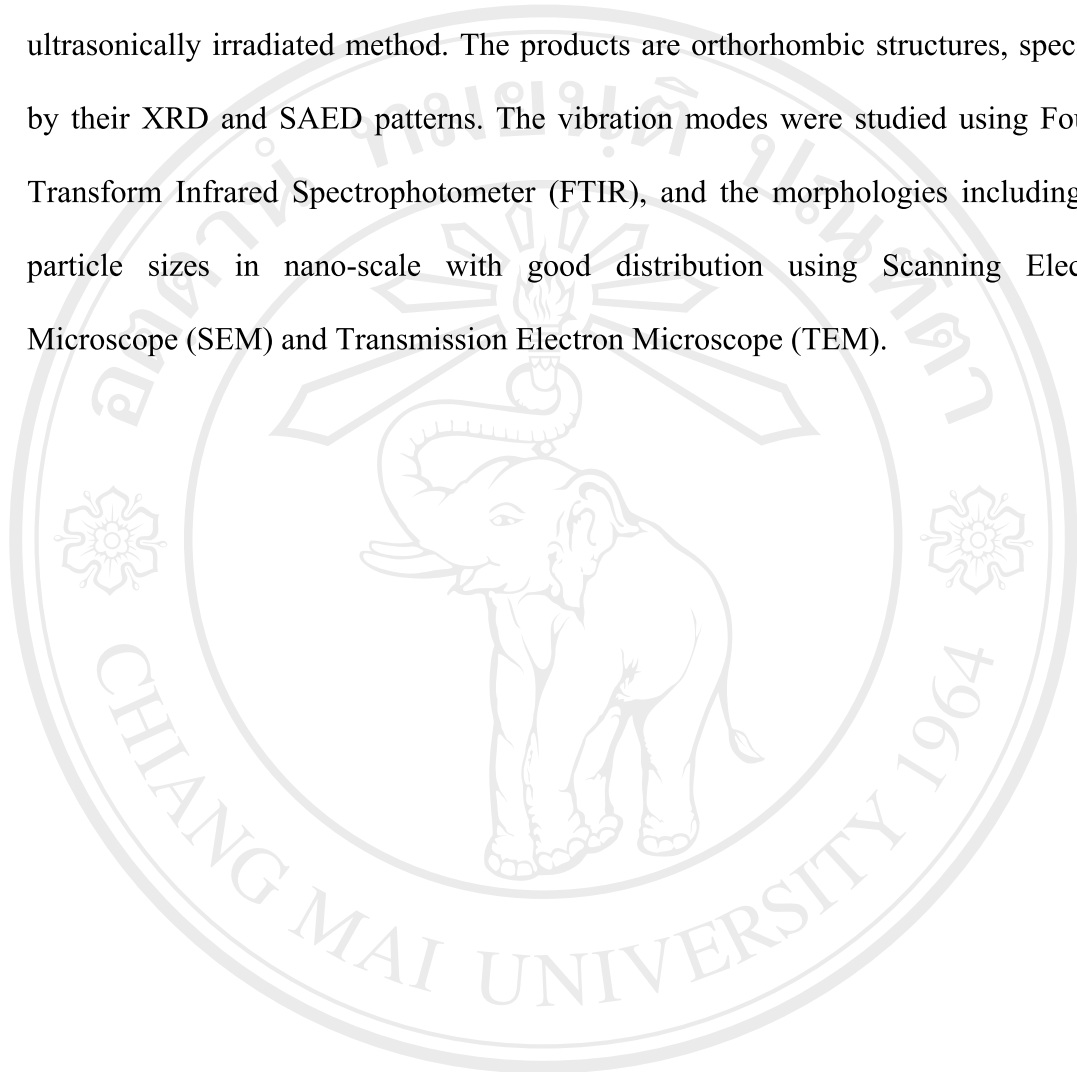
To form MCO<sub>3</sub> (M=Sr, Ba) nanoparticles, M(NO<sub>3</sub>)<sub>2</sub> reacted with Na<sub>2</sub>CO<sub>3</sub> in ethylene glycol (EG) under ultrasonic irradiation (UIRR) by the reaction



Once the MCO<sub>3</sub> nuclei formed in ethylene glycol by the assistance of ultrasonic irradiation, they did not fully develop. They grew into a number of nanoparticles via the diffusion process in EG. These nanoparticles became larger when the lengths of times were longer. They were still retaining their nanosize, although the reaction time was lengthened to 5 h. Comparing to the works of Alavi and Morsali [73,74], Sr(CH<sub>3</sub>COO)<sub>2</sub> reacted with NaOH in ethanol with the aid of ultrasonic irradiation to form precursors (Sr(OH)<sub>2</sub>.H<sub>2</sub>O, Sr(OH)<sub>2</sub>.8H<sub>2</sub>O and SrCO<sub>3</sub> mixtures), which were subsequently calcined at 400 °C to form SrCO<sub>3</sub> [73]. When Ba(CH<sub>3</sub>COO)<sub>2</sub> instead of Sr(CH<sub>3</sub>COO)<sub>2</sub> was used BaCO<sub>3</sub> nanostructures were synthesized without the requirement of calcination [74].

### 5.5 Conclusion of SrCO<sub>3</sub> and BaCO<sub>3</sub> using a sonochemical method

SrCO<sub>3</sub> and BaCO<sub>3</sub> nanocrystallines were successfully synthesized by the ultrasonically irradiated method. The products are orthorhombic structures, specified by their XRD and SAED patterns. The vibration modes were studied using Fourier Transform Infrared Spectrophotometer (FTIR), and the morphologies including the particle sizes in nano-scale with good distribution using Scanning Electron Microscope (SEM) and Transmission Electron Microscope (TEM).



ลิขสิทธิ์มหาวิทยาลัยเชียงใหม่  
Copyright© by Chiang Mai University  
All rights reserved

## APPENDIX B

### The Joint Committee for Powder Diffraction Standards (JCPDS)

#### 1. Silver Bismuth Sulfide, JCPDS file number 04-0699

##### Name and formula

|                    |                        |
|--------------------|------------------------|
| Reference code:    | 04-0699                |
| PDF index name:    | Silver Bismuth Sulfide |
| Empirical formula: | AgBiS <sub>2</sub>     |
| Chemical formula:  | AgBiS <sub>2</sub>     |

##### Crystallographic parameters

|                 |         |
|-----------------|---------|
| Crystal system: | Cubic   |
| a (?):          | 5.6460  |
| b (?):          | 5.6460  |
| c (?):          | 5.6460  |
| Alpha (?):      | 90.0000 |
| Beta (?):       | 90.0000 |
| Gamma (?):      | 90.0000 |

Volume of cell: 179.98

RIR: -

##### Status, subfiles and quality

|           |                           |
|-----------|---------------------------|
| Status:   | Marked as deleted by ICDD |
| Subfiles: | Inorganic                 |
| Quality:  | Blank (B)                 |

##### Comments

Color: Reddish-black

General comments: Hydrosynthesized in a pressure bomb.

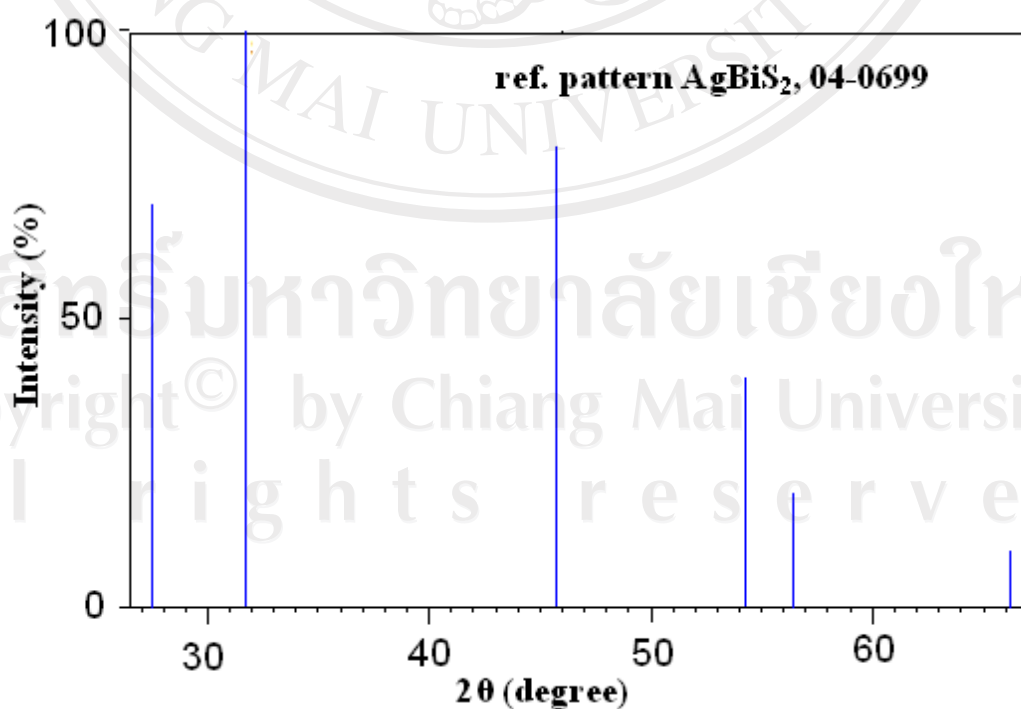
### References

Primary reference: Graham., *Am. Mineral.*, **36**, 448, (1951)

### Peak list

| No. | h | k | l | d [Å]   | I [%] |
|-----|---|---|---|---------|-------|
| 1   | 1 | 1 | 1 | 3.24000 | 70.0  |
| 2   | 2 | 0 | 0 | 2.82000 | 100.0 |
| 3   | 2 | 2 | 0 | 1.98000 | 80.0  |
| 4   | 3 | 1 | 1 | 1.69000 | 40.0  |
| 5   | 2 | 2 | 2 | 1.63000 | 20.0  |
| 6   | 4 | 0 | 0 | 1.41000 | 10.0  |

### Stick Pattern



## 2. Bismuth Sulfide, JCPDS file number 17-0320

### Name and formula

|                    |                         |
|--------------------|-------------------------|
| Reference code:    | 17-0320                 |
| Mineral name:      | Bismuthinite, syn       |
| PDF index name:    | Bismuth Sulfide         |
| Empirical formula: | $\text{Bi}_2\text{S}_3$ |
| Chemical formula:  | $\text{Bi}_2\text{S}_3$ |

### Crystallographic parameters

|                     |              |
|---------------------|--------------|
| Crystal system:     | Orthorhombic |
| Space group:        | Pbnm         |
| Space group number: | 62           |
| a (?):              | 11.1490      |
| b (?):              | 11.3040      |
| c (?):              | 3.9810       |
| Alpha (?):          | 90.0000      |
| Beta (?):           | 90.0000      |
| Gamma (?):          | 90.0000      |
| Calculated density: | 6.81         |
| Measured density:   | 6.78         |
| Volume of cell:     | 501.72       |
| Z:                  | 4.00         |
| RIR:                | 2.10         |



**Subfiles and Quality**

|                          |   |
|--------------------------|---|
| Subfiles:                | Inorganic<br>Mineral<br>Alloy, metal or intermetallic<br>Common Phase<br>Educational pattern<br>Forensic<br>NBS pattern |
| Quality:                 | Indexed (I)   |
| <b><u>Comments</u></b>   |   |
| Color:                   | Dark gray   |
| General comments:        | Measured density from <i>Dana's System of Mineralogy</i> ,<br><i>7th Ed.</i> , II 962.                                  |
| Sample source:           | Sample prepared by Glatz, A., Carrier Research and<br>Development Co.   |
| Additional pattern:      | Validated by calculated pattern 42-541.<br>See ICSD 201066 (PDF 84-279).  |
| Temperature:             | Pattern taken at 25 C.  |
| <b><u>References</u></b> |   |
| Primary reference:       | <i>Natl. Bur. Stand. (U.S.) Monogr.</i> 25, 5, 13, (1967)   |
| Structure:               | Mumme, W., Watts, J., <i>Can. Mineral.</i> , 14, 322, (1976)  |

**Peak list**

| No. | h | k | l | d [Å] | I [%] |
|-----|---|---|---|-------|-------|
|-----|---|---|---|-------|-------|

|    |   |   |   |         |       |
|----|---|---|---|---------|-------|
| 1  | 1 | 1 | 0 | 7.93600 | 2.0   |
| 2  | 0 | 2 | 0 | 5.60400 | 20.0  |
| 3  | 2 | 0 | 0 | 5.56600 | 6.0   |
| 4  | 1 | 2 | 0 | 5.04000 | 20.0  |
| 5  | 2 | 2 | 0 | 3.96700 | 40.0  |
| 6  | 1 | 0 | 1 | 3.74800 | 18.0  |
| 7  | 1 | 3 | 0 | 3.56900 | 100.0 |
| 8  | 3 | 1 | 0 | 3.53000 | 60.0  |
| 9  | 0 | 2 | 1 | 3.25300 | 16.0  |
| 10 | 2 | 1 | 1 | 3.11800 | 80.0  |
| 11 | 0 | 4 | 0 | 2.82400 | 14.0  |
| 12 | 2 | 2 | 1 | 2.81200 | 50.0  |
| 13 | 3 | 0 | 1 | 2.71700 | 30.0  |
| 14 | 4 | 1 | 0 | 2.70900 | 4.0   |
| 15 | 3 | 1 | 1 | 2.64100 | 18.0  |
| 16 | 2 | 4 | 0 | 2.52100 | 40.0  |
| 17 | 4 | 2 | 0 | 2.49900 | 12.0  |
| 18 | 2 | 3 | 1 | 2.45600 | 10.0  |
| 19 | 0 | 4 | 1 | 2.30500 | 20.0  |
| 20 | 1 | 4 | 1 | 2.25800 | 30.0  |
| 21 | 4 | 3 | 0 | 2.24100 | 12.0  |
| 22 | 5 | 1 | 0 | 2.18800 | 6.0   |

ลิขสิทธิ์ภาพวิทยาลัยเชียงใหม่  
 Copyright © by Chiang Mai University  
 All rights reserved

| <b>No.</b> | <b>h</b> | <b>k</b> | <b>l</b> | <b>d [Å]</b> | <b>I [%]</b> |
|------------|----------|----------|----------|--------------|--------------|
| 23         | 2        | 4        | 1        | 2.13000      | 8.0          |
| 24         | 4        | 2        | 1        | 2.11800      | 10.0         |
| 25         | 2        | 5        | 0        | 2.09600      | 10.0         |
| 26         | 5        | 2        | 0        | 2.07500      | 10.0         |
| 27         | 0        | 0        | 2        | 1.99000      | 18.0         |
| 28         | 4        | 4        | 0        | 1.98500      | 16.0         |
| 29         | 4        | 3        | 1        | 1.95300      | 40.0         |
| 30         | 5        | 0        | 1        | 1.94500      | 30.0         |
| 31         | 1        | 5        | 1        | 1.93700      | 16.0         |
| 32         | 3        | 5        | 0        | 1.93200      | 10.0         |
| 33         | 5        | 3        | 0        | 1.91900      | 18.0         |
| 34         | 0        | 6        | 0        | 1.88400      | 25.0         |
| 35         | 1        | 6        | 0        | 1.85700      | 14.0         |
| 36         | 2        | 5        | 1        | 1.85300      | 16.0         |
| 37         | 6        | 1        | 0        | 1.83400      | 10.0         |
| 38         | 2        | 6        | 0        | 1.78500      | 4.0          |
| 39         | 2        | 2        | 2        | 1.78000      | 8.0          |
| 40         | 6        | 2        | 0        | 1.76500      | 6.0          |
| 41         | 5        | 4        | 0        | 1.75000      | 8.0          |
| 42         | 3        | 5        | 1        | 1.73800      | 35.0         |
| 43         | 3        | 1        | 2        | 1.73400      | 14.0         |
| 44         | 0        | 6        | 1        | 1.70300      | 10.0         |
| 45         | 1        | 6        | 1        | 1.68300      | 5.0          |

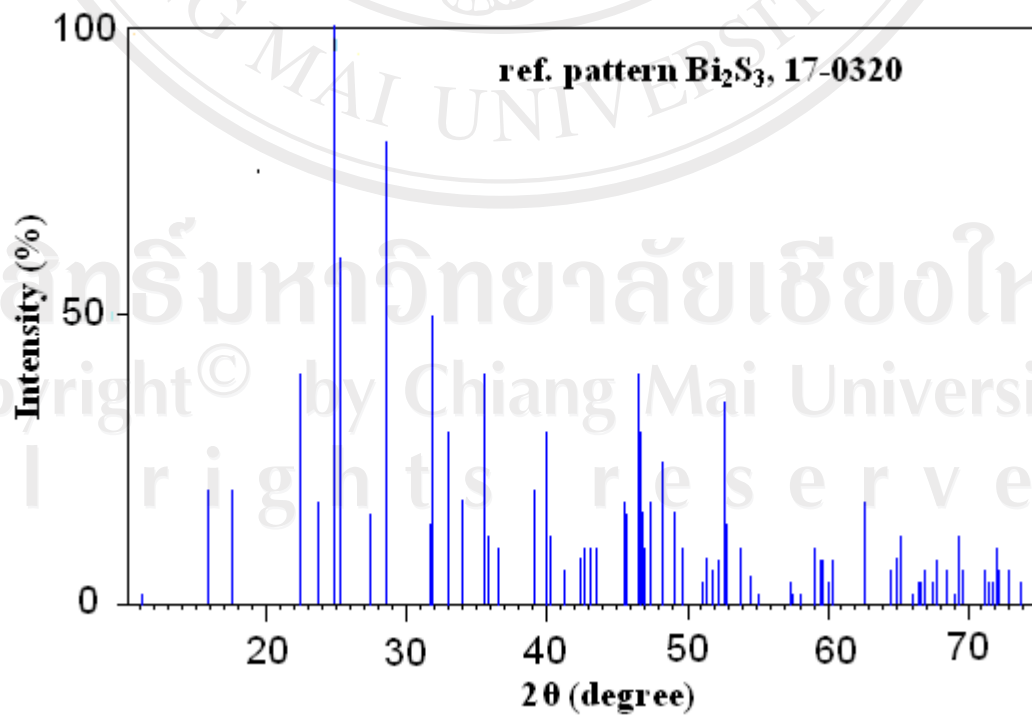
ลิขสิทธิ์มหาวิทยาลัยเชียงใหม่  
 Copyright © by Chiang Mai University  
 All rights reserved

| <b>No.</b> | <b>h</b> | <b>k</b> | <b>l</b> | <b>d [Å]</b> | <b>I [%]</b> |
|------------|----------|----------|----------|--------------|--------------|
| 46         | 3        | 6        | 0        | 1.68000      | 4.0          |
| 47         | 6        | 1        | 1        | 1.66500      | 2.0          |
| 48         | 4        | 5        | 1        | 1.60600      | 4.0          |
| 49         | 4        | 1        | 2        | 1.60300      | 2.0          |
| 50         | 5        | 5        | 0        | 1.58700      | 2.0          |
| 51         | 2        | 4        | 2        | 1.56200      | 10.0         |
| 52         | 6        | 4        | 0        | 1.55200      | 8.0          |
| 53         | 3        | 6        | 1        | 1.54800      | 8.0          |
| 54         | 6        | 3        | 1        | 1.53700      | 4.0          |
| 55         | 7        | 2        | 0        | 1.53280      | 8.0          |
| 56         | 1        | 7        | 1        | 1.48280      | 10.0         |
| 57         | 1        | 5        | 2        | 1.48090      | 18.0         |
| 58         | 2        | 7        | 1        | 1.44510      | 6.0          |
| 59         | 2        | 5        | 2        | 1.44310      | 6.0          |
| 60         | 5        | 2        | 2        | 1.43590      | 8.0          |
| 61         | 7        | 2        | 1        | 1.43060      | 12.0         |
| 62         | 0        | 8        | 0        | 1.41270      | 2.0          |
| 63         | 4        | 4        | 2        | 1.40520      | 4.0          |
| 64         | 1        | 8        | 0        | 1.40180      | 4.0          |
| 65         | 4        | 7        | 0        | 1.39740      | 6.0          |
| 66         | 3        | 5        | 2        | 1.38620      | 4.0          |
| 67         | 8        | 1        | 0        | 1.38300      | 4.0          |
| 68         | 5        | 3        | 2        | 1.38140      | 8.0          |

ลิขสิทธิ์มหาวิทยาลัยเชียงใหม่  
 Copyright © by Chiang Mai University  
 All rights reserved

| No. | h | k | l | d [Å]   | I [%] |
|-----|---|---|---|---------|-------|
| 69  | 0 | 6 | 2 | 1.36820 | 6.0   |
| 70  | 1 | 6 | 2 | 1.35800 | 2.0   |
| 71  | 5 | 6 | 1 | 1.35340 | 12.0  |
| 72  | 6 | 5 | 1 | 1.34980 | 6.0   |
| 73  | 6 | 6 | 0 | 1.32250 | 6.0   |
| 74  | 4 | 7 | 1 | 1.31840 | 4.0   |
| 75  | 5 | 4 | 2 | 1.31450 | 4.0   |
| 76  | 7 | 4 | 1 | 1.31010 | 10.0  |
| 77  | 8 | 1 | 1 | 1.30620 | 6.0   |
| 78  | 2 | 8 | 1 | 1.29500 | 6.0   |
| 79  | 2 | 1 | 3 | 1.28280 | 4.0   |

**Stick Pattern**



### 3. Strontium Carbonate, JCPDS file number 05-0418

#### Name and formula

|                    |                     |
|--------------------|---------------------|
| Reference code:    | 05-0418             |
| Mineral name:      | Strontianite, syn   |
| PDF index name:    | Strontium Carbonate |
| Empirical formula: | CO <sub>3</sub> Sr  |
| Chemical formula:  | SrCO <sub>3</sub>   |

#### Crystallographic parameters

|                     |              |
|---------------------|--------------|
| Crystal system:     | Orthorhombic |
| Space group:        | Pmcn         |
| Space group number: | 62           |
| a (?):              | 5.1070       |
| b (?):              | 8.4140       |
| c (?):              | 6.0290       |
| Alpha (?):          | 90.0000      |
| Beta (?):           | 90.0000      |
| Gamma (?):          | 90.0000      |
| Calculated density: | 3.79         |
| Measured density:   | 3.76         |
| Volume of cell:     | 259.07       |
| Z:                  | 4.00         |
| RIR:                | -            |



**Subfiles and Quality**

Subfiles: Inorganic  
 Mineral  
 Common Phase  
 Educational pattern  
 Forensic  
 NBS pattern  
 Superconducting Material  
 Quality: Star (S)

**Comments**

Color: Colorless

General comments: There is also a rhombohedral form of  $\text{SrCO}_3$  stable above 912 C.

Sample source: Sample from Mallinckrodt Chemical Works.

Analysis: Spectroscopic analysis: <0.1% Ba; 0.01% Ca, Li;

<0.001% Al, K, Mn, Na; <0.0001% Cu, Fe, Mg, Si.

Optical data:

$A=1.517$ ,  $B=1.663$ ,  $Q=1.667$ ,  $\text{Sign}=-$ ,  $2V=18^\circ$ (calc.)

Additional pattern:

To replace 1-556 and 2-397.

See ICSD 15195, 27293 and 202793 (PDF 71-2393, 74-1491 and 84-1778).

Temperature:

Pattern taken at 26 C.

**References**

Primary reference: Swanson, Fuyat., *Natl. Bur. Stand. (U.S.), Circ. 539*,  
**III, 56, (1954)**

**Peak list**

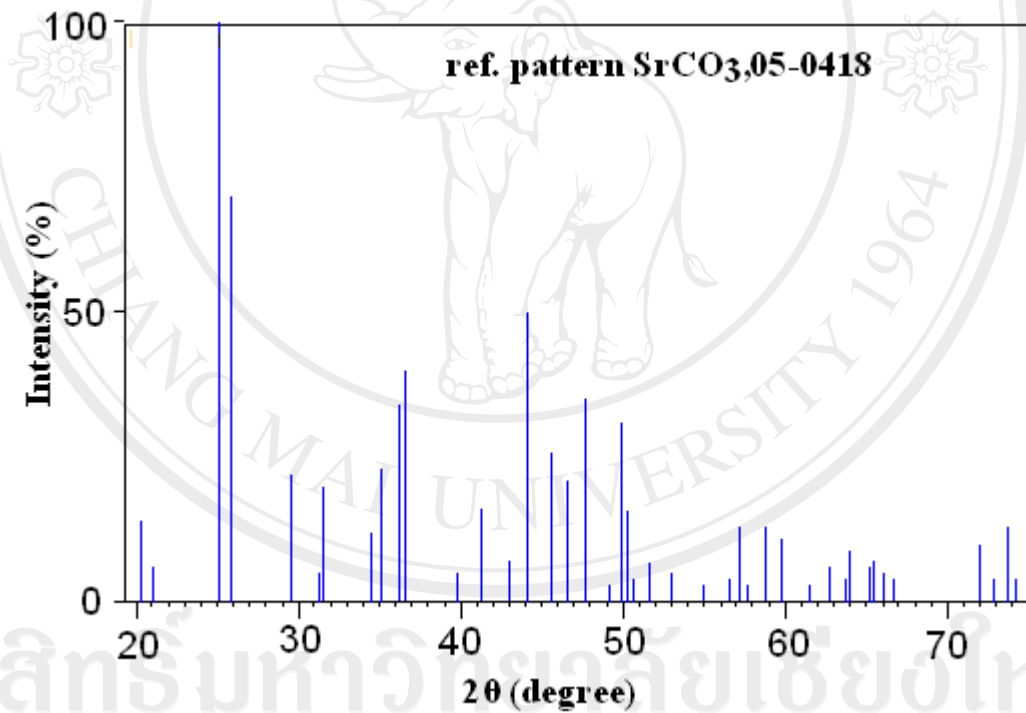
| <b>No.</b> | <b>h</b> | <b>k</b> | <b>l</b> | <b>d [Å]</b> | <b>I [%]</b> |
|------------|----------|----------|----------|--------------|--------------|
| 1          | 1        | 1        | 0        | 4.36700      | 14.0         |
| 2          | 0        | 2        | 0        | 4.20700      | 6.0          |
| 3          | 1        | 1        | 1        | 3.53500      | 100.0        |
| 4          | 0        | 2        | 1        | 3.45000      | 70.0         |
| 5          | 0        | 0        | 2        | 3.01400      | 22.0         |
| 6          | 1        | 2        | 1        | 2.85900      | 5.0          |
| 7          | 0        | 1        | 2        | 2.83800      | 20.0         |
| 8          | 1        | 0        | 2        | 2.59600      | 12.0         |
| 9          | 2        | 0        | 0        | 2.55400      | 23.0         |
| 10         | 1        | 1        | 2        | 2.48100      | 34.0         |
| 11         | 1        | 3        | 0        | 2.45800      | 40.0         |
| 12         | 0        | 2        | 2        | 2.45110      | 33.0         |
| 13         | 2        | 1        | 1        | 2.26460      | 5.0          |
| 14         | 2        | 2        | 0        | 2.18310      | 16.0         |
| 15         | 0        | 4        | 0        | 2.10350      | 7.0          |

| <b>No.</b> | <b>h</b> | <b>k</b> | <b>l</b> | <b>d [Å]</b> | <b>I [%]</b> |
|------------|----------|----------|----------|--------------|--------------|
| 16         | 2        | 2        | 1        | 2.05260      | 50.0         |
| 17         | 0        | 4        | 1        | 1.98600      | 26.0         |
| 18         | 2        | 0        | 2        | 1.94890      | 21.0         |
| 19         | 1        | 3        | 2        | 1.90530      | 35.0         |
| 20         | 1        | 4        | 1        | 1.85140      | 3.0          |
| 21         | 1        | 1        | 3        | 1.82530      | 31.0         |
| 22         | 0        | 2        | 3        | 1.81340      | 16.0         |
| 23         | 2        | 3        | 1        | 1.80230      | 4.0          |
| 24         | 2        | 2        | 2        | 1.76850      | 7.0          |
| 25         | 0        | 4        | 2        | 1.72530      | 5.0          |
| 26         | 3        | 1        | 0        | 1.66840      | 3.0          |
| 27         | 2        | 4        | 0        | 1.62360      | 4.0          |
| 28         | 3        | 1        | 1        | 1.60800      | 13.0         |
| 29         | 1        | 5        | 0        | 1.59810      | 3.0          |
| 30         | 2        | 4        | 1        | 1.56760      | 13.0         |
| 31         | 1        | 5        | 1        | 1.54470      | 11.0         |
| 32         | 0        | 0        | 4        | 1.50720      | 3.0          |
| 33         | 2        | 2        | 3        | 1.47820      | 6.0          |
| 34         | 3        | 1        | 2        | 1.45960      | 4.0          |
| 35         | 3        | 3        | 0        | 1.45510      | 9.0          |
| 36         | 2        | 4        | 2        | 1.42930      | 6.0          |
| 37         | 1        | 1        | 4        | 1.42460      | 7.0          |
| 38         | 1        | 5        | 2        | 1.41200      | 5.0          |

ลิขสิทธิ์มหาวิทยาลัยเชียงใหม่  
 Copyright © by Chiang Mai University  
 All rights reserved

| No. | h | k | l | d [Å]   | I [%] |
|-----|---|---|---|---------|-------|
| 39  | 0 | 6 | 0 | 1.40240 | 4.0   |
| 40  | 3 | 3 | 2 | 1.31030 | 10.0  |
| 41  | 2 | 0 | 4 | 1.29770 | 4.0   |
| 42  | 3 | 1 | 3 | 1.28400 | 13.0  |
| 43  | 4 | 0 | 0 | 1.27660 | 4.0   |

**Stick Pattern**



ลิขสิทธิ์มหาวิทยาลัยเชียงใหม่  
 Copyright© by Chiang Mai University  
 All rights reserved

#### 4. Barium Carbonate, JCPDS file number 05-0378

##### Name and formula

|                    |                   |
|--------------------|-------------------|
| Reference code:    | 05-0378           |
| Mineral name:      | Witherite, syn    |
| PDF index name:    | Barium Carbonate  |
| Empirical formula: | BaCO <sub>3</sub> |
| Chemical formula:  | BaCO <sub>3</sub> |

##### Crystallographic parameters

|                     |              |
|---------------------|--------------|
| Crystal system:     | Orthorhombic |
| Space group:        | Pmcn         |
| Space group number: | 62           |
| a (?):              | 5.3140       |
| b (?):              | 8.9040       |
| c (?):              | 6.4300       |
| Alpha (?):          | 90.0000      |
| Beta (?):           | 90.0000      |
| Gamma (?):          | 90.0000      |
| Calculated density: | 4.31         |
| Volume of cell:     | 304.24       |
| Z:                  | 4.00         |
| RIR:                | 4.20         |

**Subfiles and Quality**

|                        |   |
|------------------------|---|
| Subfiles:              | Inorganic   |
|                        | Mineral   |
|                        | Common Phase  |
|                        | Educational pattern   |
|                        | Forensic  |
|                        | NBS pattern   |
|                        | Superconducting Material  |
| Quality:               | Indexed (I)   |
| <b><u>Comments</u></b> |   |
| Color:                 | Colorless   |
| Sample source:         | Sample from Mallinckrodt Chemical Works.                                      |
| Analysis:              | Spectroscopic analysis: showed <0.01% Al, Ca, Na, Sr; <0.001% Cu, Fe, Mg, Pb. |
| Optical data:          | A=1.530, B=1.679, Q=1.680, Sign=-, 2V=9(calc.)                                |
| Additional pattern:    | To replace 1-506.   |
| Temperature:           | Pattern taken at 26 C.  |

**References**

|                    |  |
|--------------------|--|
| Primary reference: | Swanson, Fuyat., <i>Natl. Bur. Stand. (U.S.), Circ. 539</i> , II, 54, (1953) |
|--------------------|--|

**Peak list**

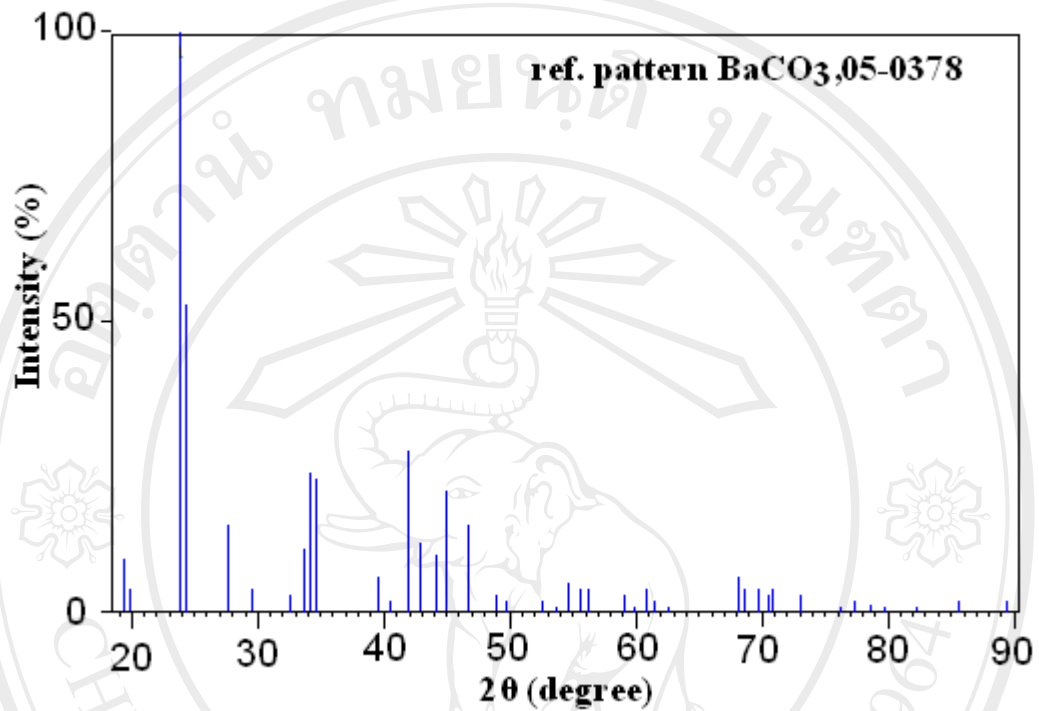
|    |   |   |   |         |       |
|----|---|---|---|---------|-------|
| 1  | 1 | 1 | 0 | 4.56000 | 9.0   |
| 2  | 0 | 2 | 0 | 4.45000 | 4.0   |
| 3  | 1 | 1 | 1 | 3.72000 | 100.0 |
| 4  | 0 | 2 | 1 | 3.66000 | 53.0  |
| 5  | 0 | 0 | 2 | 3.21500 | 15.0  |
| 6  | 0 | 1 | 2 | 3.02500 | 4.0   |
| 7  | 1 | 0 | 2 | 2.74900 | 3.0   |
| 8  | 2 | 0 | 0 | 2.65600 | 11.0  |
| 9  | 1 | 1 | 2 | 2.62800 | 24.0  |
| 10 | 1 | 3 | 0 | 2.59000 | 23.0  |
| 11 | 2 | 2 | 0 | 2.28100 | 6.0   |
| 12 | 0 | 4 | 0 | 2.22600 | 2.0   |
| 13 | 2 | 2 | 1 | 2.15000 | 28.0  |
| 14 | 0 | 4 | 1 | 2.10400 | 12.0  |
| 15 | 2 | 0 | 2 | 2.04800 | 10.0  |
| 16 | 1 | 3 | 2 | 2.01900 | 21.0  |
| 17 | 1 | 1 | 3 | 1.94000 | 15.0  |
| 18 | 2 | 2 | 2 | 1.85900 | 3.0   |
| 19 | 0 | 4 | 2 | 1.83000 | 2.0   |
| 20 | 3 | 1 | 0 | 1.73700 | 2.0   |
| 21 | 2 | 4 | 0 | 1.70600 | 1.0   |
| 22 | 3 | 1 | 1 | 1.67700 | 5.0   |
| 23 | 2 | 4 | 1 | 1.64900 | 4.0   |

ลิขสิทธิ์มหาวิทยาลัยเชียงใหม่  
 Copyright © by Chiang Mai University  
 All rights reserved



**No. h k l d [Å] I [%]**

|    |   |   |   |         |     |
|----|---|---|---|---------|-----|
| 24 | 1 | 5 | 1 | 1.63300 | 4.0 |
| 25 | 2 | 2 | 3 | 1.56300 | 3.0 |
| 26 | 0 | 4 | 3 | 1.54300 | 1.0 |
| 27 | 3 | 3 | 0 | 1.52100 | 4.0 |
| 28 | 2 | 4 | 2 | 1.50800 | 2.0 |
| 29 | 0 | 6 | 0 | 1.48400 | 1.0 |
| 30 | 3 | 3 | 2 | 1.37500 | 6.0 |
| 31 | 1 | 3 | 4 | 1.36600 | 4.0 |
| 32 | 0 | 6 | 2 | 1.34800 | 4.0 |
| 33 | 2 | 4 | 3 | 1.33500 | 3.0 |
| 34 | 4 | 0 | 0 | 1.32800 | 4.0 |
| 35 | 2 | 6 | 0 | 1.29500 | 3.0 |
| 36 | 2 | 3 | 4 | 1.24800 | 1.0 |
| 37 | 3 | 5 | 1 | 1.23300 | 2.0 |
| 38 | 1 | 7 | 1 | 1.21500 | 1.0 |
| 39 | 1 | 2 | 5 | 1.20200 | 1.0 |
| 40 | 2 | 4 | 4 | 1.17030 | 1.0 |
| 41 | 4 | 3 | 2 | 1.13350 | 2.0 |
| 42 | 0 | 8 | 1 | 1.09510 | 2.0 |

Stick Pattern

ลิขสิทธิ์มหาวิทยาลัยเชียงใหม่  
Copyright© by Chiang Mai University  
All rights reserved

## APPENDIX C

### Camera constant used for the indexing of SAED pattern

Table appendix c. TEM constant ( $L\lambda$ ) at 200 kV

| L (cm) | $D_{111}\text{Au}$ (mm) | $r_{111}\text{Au}$ (mm) | $D_{111}\text{Auv}$ (Å) | $L\lambda$ (mm.Å) |
|--------|-------------------------|-------------------------|-------------------------|-------------------|
| 40     | 8.70                    | 4.35                    | 2.355                   | 10.2442           |
| 60     | 13.2                    | 6.60                    | 2.355                   | 15.5430           |
| 80     | 17.2                    | 8.60                    | 2.355                   | 20.2530           |
| 100    | 21.2                    | 10.60                   | 2.355                   | 24.9630           |
| 120    | 25.2                    | 12.60                   | 2.355                   | 29.6730           |
| 150    | 31.5                    | 15.75                   | 2.355                   | 37.0912           |
| 200    | 41.5                    | 20.75                   | 2.355                   | 48.8662           |
| 250    | 51.8                    | 25.90                   | 2.355                   | 60.9945           |



**APPENDIX D**

**International publications**

ลิขสิทธิ์มหาวิทยาลัยเชียงใหม่

Copyright© by Chiang Mai University

All rights reserved



## Characterization of AgBiS<sub>2</sub> nanostructured flowers produced by solvothermal reaction

Titipun Thongtem<sup>a,\*</sup>, Narongrit Tipcompor<sup>a</sup>, Somchai Thongtem<sup>b</sup>

<sup>a</sup> Department of Chemistry, Faculty of Science, Chiang Mai University, Chiang Mai 50200, Thailand

<sup>b</sup> Department of Physics and Materials Science, Faculty of Science, Chiang Mai University, Chiang Mai 50200, Thailand

### ARTICLE INFO

#### Article history:

Received 18 September 2009

Accepted 1 January 2010

Available online 7 January 2010

#### Keywords:

Characterization methods

Electron microscopy

X-ray techniques

Luminescence

### ABSTRACT

AgBiS<sub>2</sub> nanostructured flowers were produced from CH<sub>3</sub>COOAg, Bi(NO<sub>3</sub>)<sub>3</sub>·5H<sub>2</sub>O and thiosemicarbazide (NH<sub>2</sub>CSNHNH<sub>2</sub>) using different solvents [ethylene glycol (EG), water (H<sub>2</sub>O), polyethylene glycol with molecular weight of 200 (PEG200), and propylene glycol (PG)] in Teflon-lined stainless steel autoclaves. The phase and purity were detected using X-ray diffraction (XRD), controlled by the solvents. The product was purified AgBiS<sub>2</sub> produced by the 200 °C and 24 h reaction in EG, corresponding to selected area electron diffraction (SAED) and simulation patterns. Scanning and transmission electron microscopies (SEM and TEM) revealed the formation of nanostructured flowers – enlarged by the increase in the lengths of time and temperature. Their photoluminescence (PL) emissions were detected at the same wavelength of 382 nm (3.24 eV), although they were produced under different conditions.

© 2010 Elsevier B.V. All rights reserved.

### 1. Introduction

Presently, energy saving is one of the top policies of humans in all parts of the world. Thus a number of scientists and engineers pay much attention on different processes for large scale productions. Solvothermal and hydrothermal reactions are very appropriate for such of these; especially, for materials with nanostructured flowers. AgBiS<sub>2</sub>, one of the semiconducting ternary sulfides, has been very attractive, due to its linear and non-linear properties [1,2]. It has high potential to use as optoelectronic and thermoelectric devices, including optical recording media [1,2]. To the best of our knowledge, there are not many reports on the synthesis of AgBiS<sub>2</sub> with different morphologies. Among them are dendrites by microwave synthesis [1], nanorods and coral-shaped crystals by a polyol route [2,3], and flowers and hexapods by cyclic microwave-assisted synthesis [4]. For the present research, production of purified AgBiS<sub>2</sub> nanostructured flowers using the solvothermal process was studied and reported.

### 2. Experiment

To produce nanostructured AgBiS<sub>2</sub>, 0.003 mol CH<sub>3</sub>COOAg, 0.003 mol Bi(NO<sub>3</sub>)<sub>3</sub>·5H<sub>2</sub>O and 0.006 mol thiosemicarbazide (NH<sub>2</sub>CSNHNH<sub>2</sub>) were separately dissolved in different solvents [ethylene glycol (EG), water (H<sub>2</sub>O), polyethylene glycol with molecular weight of 200 (PEG200), and

propylene glycol (PG)]. The Ag<sup>+</sup> and Bi<sup>3+</sup> solutions were mixed to form a mixture, to which the thiosemicarbazide solution was subsequently added. Volumes of each mixture were adjusted to be 50 ml, with 10 min stirring. The chemical reactions proceeded at 140–200 °C for 24–72 h, in tightly closed stainless steel autoclaves lined with Teflon. Finally, black precipitates were produced, separated by filtration, washed with de-ionized water and absolute ethanol, and dried at 70 °C for 24 h. The products were characterized to determine their phase(s), purity, morphologies and emissions.

### 3. Results and discussion

Fig. 1 shows XRD spectra of the products produced in the autoclaves under different conditions. At 200 °C for 24 h in different solvents (Fig. 1a), the products were specified as cubic AgBiS<sub>2</sub> (JCPDS no. 04-0699) [5] with some Bi<sub>2</sub>S<sub>3</sub> (JCPDS no. 17-0320) [5] as the impurity – excluding that produced in EG. To save energy consumption, the solvothermal temperature was reduced in a series of steps from 200 °C to 140 °C. It was found that the XRD peaks (Fig. 1b) for the production in EG became broadened – the crystalline degrees of these pure products became lower. These products were no longer pure, when the temperature was lower than 180 °C – some Bi<sub>2</sub>S<sub>3</sub> impurity was also detected. At 200 °C and longer time in EG, XRD spectra (Fig. 1c) of the products were very sharp. They are independent of the length of time. These imply that both the purity and degree of crystallinity remain unchanged.

SEM and TEM images (Figs. 2a–c, 3a and e) show nanostructured flowers of AgBiS<sub>2</sub> produced at different temperatures and lengths of time. They are totally different from the previous report [4]. Increasing in the temperatures and lengths of time has the influence to enlarge

\* Corresponding author. Tel.: +66 53 943344; fax: +66 53 892277.

E-mail addresses: [ttphongtem@yahoo.com](mailto:ttphongtem@yahoo.com), [ttphongtem@hotmail.com](mailto:ttphongtem@hotmail.com) (T. Thongtem).

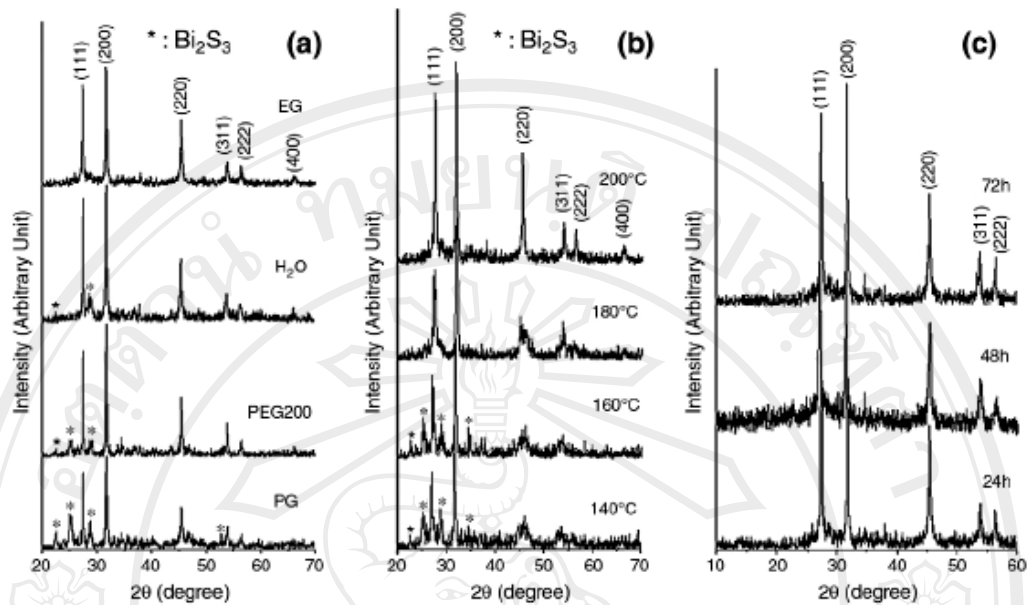


Fig. 1. XRD spectra of the products produced at (a) 200 °C for 24 h in different solvents, (b) different temperatures for 24 h in EG, and (c) 200 °C for different lengths of time in EG.

their sizes. Some petals not only became longer and larger, but also have branches. High magnification TEM image (Fig. 3c) of a petal produced at 200 °C for 24 h shows a number of parallel lattice planes with 3.19 Å apart, corresponding to the (111) crystallographic plane of the product. A SAED pattern (Fig. 3b) of the product with 200 °C and 24 h reaction composed of a number of bright spots, arranged in concentric circles. These circles are diffuse and hollow, implying that the product is poly-nanocrystals. Another SAED pattern

(Fig. 3d), which is in good accordance with that of the simulation [6] – systematic and symmetric array of dark spots (Fig. 3f), appears as light spots of diffraction electrons from a single crystal with the  $[-112]$  direction as zone axis. They (Fig. 3b and d) were indexed [7] and specified as cubic  $\text{AgBiS}_2$  (JCPDS no. 04-0699) [5].

To produce  $\text{AgBiS}_2$ ,  $\text{CH}_3\text{COOAg}$  and  $\text{Bi}(\text{NO}_3)_3 \cdot 5\text{H}_2\text{O}$  in ethylene glycol (EG) were mixed to form a mixture, to which thiosemicarbazide ( $\text{NH}_2\text{CSNHNH}_2$ ) in EG was subsequently added. At this stage,  $\text{Ag}^+$

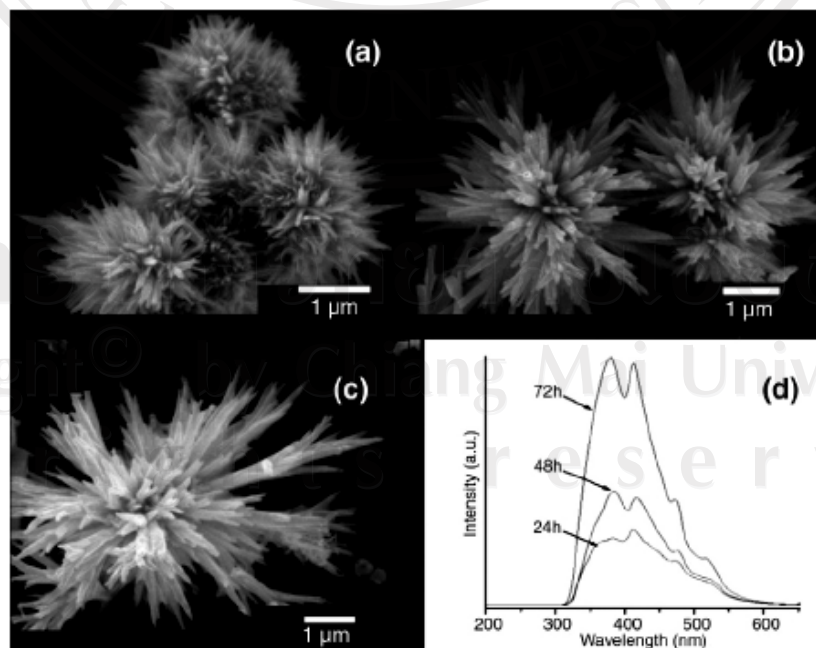


Fig. 2. SEM images of  $\text{AgBiS}_2$  produced in EG at (a) 180 °C for 24 h, (b) 200 °C for 24 h, and (c) 200 °C for 48 h. (d) PL emissions of  $\text{AgBiS}_2$  produced in EG at 200 °C for 24 h, 48 h and 72 h.



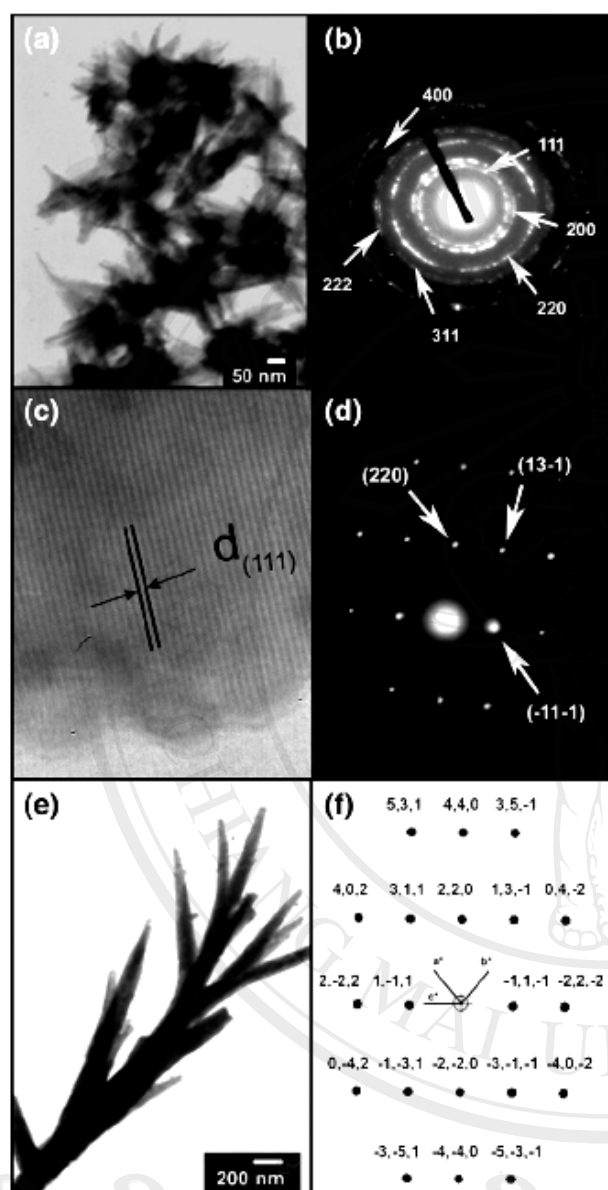
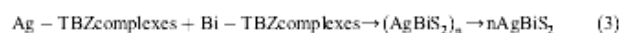


Fig. 3. TEM images and SAED patterns of  $\text{AgBiS}_2$  produced in EG at  $200^\circ\text{C}$  for (a–d) 24 h and (e) 72 h. (f) A simulated pattern comparing to (d).

and  $\text{Bi}^{3+}$  ions reacted with thiosemicarbazide (TBZ) at room temperature to form complexes [1,2].



These complexes were decomposed by the  $200^\circ\text{C}$  solvothermal reaction in EG. Due to the stability of the complexes, the reaction proceeded with rather slow rate – the number of nuclei was less than that produced by the direct ion-exchange reaction [2].  $(\text{AgBiS}_2)_n$  nuclei were produced, and finally transformed into  $\text{AgBiS}_2$  [1] – detected by XRD analysis.



The decomposition rates of these two complexes are appropriate to the production of  $\text{AgBiS}_2$  without any impurities. In general, the decomposition rates of the complexes are different, controlled by the temperatures and pressures. When the solvothermal reaction was done at lower temperature, the decomposition rates of these two complexes became slow down. The final products remain unchanged although the temperature was as low as  $180^\circ\text{C}$ . At  $200^\circ\text{C}$  and  $180^\circ\text{C}$ , molar ratio of  $\text{Ag}^+$  and  $\text{Bi}^{3+}$ , obtained from the decomposition of the complexes, was very closed to 1:1, and sulfur in the solution was either in excess or exactly right to the product formation. Thus  $\text{AgBiS}_2$  was produced and detected by XRD analysis. When the research was done at  $160^\circ\text{C}$  or  $140^\circ\text{C}$ , the decomposition rate of Ag-TBZ complexes seemed to be less than that of Bi-TBZ complexes. Thus  $\text{Ag}^+$  of the complex decomposition was used up. But for  $\text{Bi}^{3+}$  and sulfur, they were left in the solution, and additional  $\text{Bi}_2\text{S}_3$  was produced and detected. It is worth to note that  $\text{AgBiS}_2$  formation was influenced by the concentrations of  $\text{Ag}^+$ ,  $\text{Bi}^{3+}$  and sulfur obtained from the decomposition process, and the product purity was controlled by the slowest process.

When other solvents ( $\text{H}_2\text{O}$ , PEG200 and PG) instead of EG were used in the system of  $200^\circ\text{C}$  and 24 h solvothermal reaction, both  $\text{AgBiS}_2$  and  $\text{Bi}_2\text{S}_3$  were produced and detected. These imply that different temperatures and solvents played the role in the product purities.

Due to the  $200^\circ\text{C}$  and  $180^\circ\text{C}$  solvothermal reactions for 24 h in EG,  $\text{AgBiS}_2$  nanostructured flowers were produced by the orientation growth [1,2]. During growing, the process was anisotropic and the flowers were produced. As the time was lengthened, atoms had more chance to adsorb on the petals to enlarge their size. Concurrently, new young branches had also initiated to grow out from these main petals.

Photoluminescence (PL) emissions (Fig. 2d) of the products produced at  $200^\circ\text{C}$  solvothermal reaction for 24–72 h were characterized using 200 nm excitation wavelength at room temperature. Their emission peaks were detected at the same wavelengths of 382 nm (3.24 eV) with surrounding shoulders. The emission peaks were caused by the recombination of electrons and electron holes (or holes) in trapped surface states in the forbidden region [8,9], called energy band gap (or energy gap). But for the shoulders, they were caused by the shallow level of donors and acceptors between the valence and conduction bands [10]. The present result is blue shift, comparing to the 2.46 eV reflectivity of  $\text{AgBiS}_2$  compound at 295 K [11]. It is worthy of noting that emission intensities were increased with the increase in the lengths of solvothermal time. The intensities seemed to be influenced by the branching of nanostructured flowers.

#### 4. Conclusions

$\text{AgBiS}_2$  nanostructured flowers were successfully produced by the  $200^\circ\text{C}$  solvothermal reaction. The phase was detected using XRD, including SAED of which the results were in accordance with those of the simulation. SEM and TEM showed that the nanostructured flowers became larger and have branches, by increasing the length of time and temperature. Their photoluminescence (PL) emissions were detected at the same wavelength of 382 nm (3.24 eV), although the products were produced under different conditions.

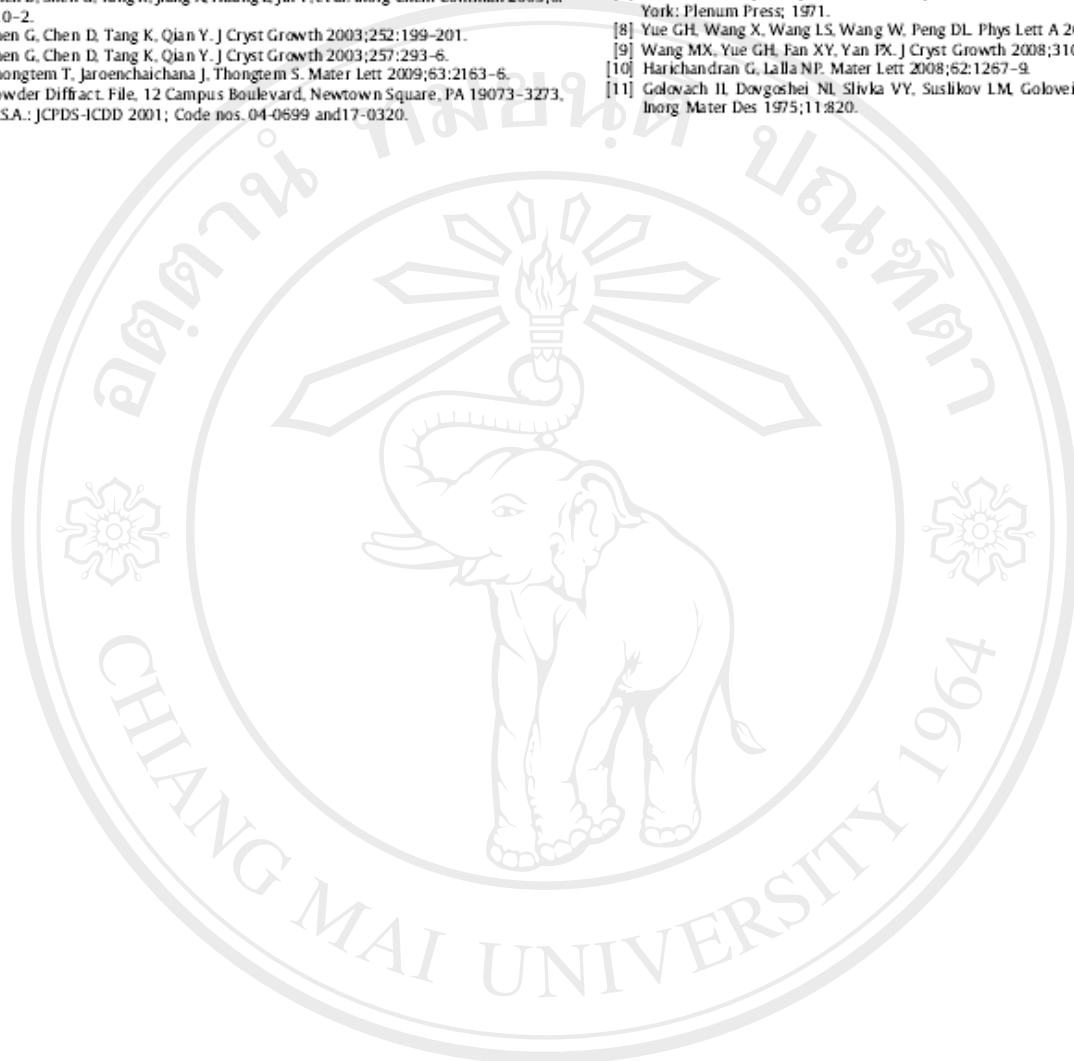
#### Acknowledgement

The research was supported under the National Research University Project for Chiang Mai University, by the Commission on Higher Education, Ministry of Education, Thailand.



## References

- [1] Chen D, Shen G, Tang K, Jiang X, Huang L, Jin Y, et al. *Inorg Chem Commun* 2003;6: 710–2.
- [2] Shen G, Chen D, Tang K, Qian Y. *J Cryst Growth* 2003;252:199–201.
- [3] Shen G, Chen D, Tang K, Qian Y. *J Cryst Growth* 2003;257:293–6.
- [4] Thongtem T, Jaroenchaichana J, Thongtem S. *Mater Lett* 2009;63:2163–6.
- [5] Powder Diffract. File, 12 Campus Boulevard, Newtown Square, PA 19073-3273, U.S.A.: JCPDS-ICDD 2001; Code nos. 04-0699 and 17-0320.
- [6] Boudias C, Monceau D. *CaRIne Crystallography* 3.1, DIVERGENT SA., Centre de Transfert, 60200 Compiègne, France; 1989–1998.
- [7] Andrews KW, Dyson DJ, Keown SR. *Interpret. Electr. Diffract. Patterns 2nd ed.*. New York: Plenum Press; 1971.
- [8] Yue GH, Wang X, Wang LS, Wang W, Peng DL. *Phys Lett A* 2008;372:5995–8.
- [9] Wang MX, Yue GH, Fan XY, Yan PX. *J Cryst Growth* 2008;310:3062–6.
- [10] Harichandran G, Lalla NP. *Mater Lett* 2008;62:1267–9.
- [11] Golovach II, Dovgoshei NI, Slivka VY, Suslikov LM, Golovei MI, Bogdanova AV. *Inorg Mater Des* 1975;11:820.



ลิขสิทธิ์มหาวิทยาลัยเชียงใหม่  
 Copyright© by Chiang Mai University  
 All rights reserved



## Characterization of SrCO<sub>3</sub> and BaCO<sub>3</sub> nanoparticles synthesized by sonochemical method

Titipun Thongtem<sup>a,\*</sup>, Narongrit Tipcompor<sup>a</sup>, Anukorn Phuruangrat<sup>b,\*</sup>, Somchai Thongtem<sup>b</sup>

<sup>a</sup> PERCH-CIC, Department of Chemistry, Faculty of Science, Chiang Mai University, Chiang Mai 50200, Thailand

<sup>b</sup> Department of Physics and Materials Science, Faculty of Science, Chiang Mai University, Chiang Mai 50200, Thailand

### ARTICLE INFO

#### Article history:

Received 2 September 2009

Accepted 23 November 2009

Available online 29 November 2009

#### Keywords:

Characterization methods

Nanomaterials

X-ray techniques

### ABSTRACT

SrCO<sub>3</sub> and BaCO<sub>3</sub> nanoparticles were synthesized using Sr(NO<sub>3</sub>)<sub>2</sub> or Ba(NO<sub>3</sub>)<sub>2</sub> and Na<sub>2</sub>CO<sub>3</sub> as starting materials in ethylene glycol by ultrasonic irradiation at 80 °C for 1–5 h. Their phases, vibration modes and morphologies were characterized using X-ray powder diffraction (XRD), Fourier transform infrared (FTIR) spectroscopy, selected area electron diffraction (SAED) and transmission electron microscopy (TEM). These products were found to be orthorhombic SrCO<sub>3</sub> and BaCO<sub>3</sub> nanoparticles with 20–50 nm and 40–100 nm ranges, respectively. Asymmetric stretching, symmetric stretching, and out of plane and in plane bending vibrations of CO<sub>3</sub><sup>2-</sup> complexes were also detected.

© 2009 Elsevier B.V. All rights reserved.

### 1. Introduction

Strontium carbonate (SrCO<sub>3</sub>) and barium carbonate (BaCO<sub>3</sub>) are very important materials for a number of industries. SrCO<sub>3</sub> is used as a constituent of ferrite magnets for small direct current motors, an additive in the production of glass for color television tubes, modern electric industries, and for the production of iridescent and special glasses, pigments, driers, paints, pyrotechnics, strontium metals and other strontium compounds [1–4]. BaCO<sub>3</sub> has also attracted attention due to its close relationship with aragonite and many important applications in ceramic and optical glass industries. It is also a highly utilized precursor for the synthesis of barium ferrites and ferroelectric materials [5,6].

In recent years, ultrasonic radiation (20 kHz–10 MHz) [5,7] has been used to prepare nanoparticles [5,7]. The chemical effects of the ultrasound arise from acoustic cavitation—formation, growth, and implosive collapse of bubbles in liquids. There are two regions of sonochemical reactivity, the inside zone of the collapsing bubble and the interface between bubbles and the liquid. The cavitation may generate very high temperature over 5000 K and pressure over 20 MPa, which enable many chemical reactions to occur. In short, during the process, the implosive collapse of bubbles generates localized hot spots through adiabatic compression or shock wave formation within the gas phase of the collapsing bubbles. These extreme conditions attained during bubble collapse have been exploited to prepare various materials with different morphologies [7,8].

In our work, SrCO<sub>3</sub> and BaCO<sub>3</sub> nanoparticles were synthesized by sonochemical method using strontium nitrate or barium nitrate and sodium carbonate as starting materials at 80 °C for 1–5 h.

### 2. Experimental procedure

BaCO<sub>3</sub> and SrCO<sub>3</sub> nanocrystallines were synthesized by the reactions of 0.005 mol of Ba(NO<sub>3</sub>)<sub>2</sub> or Sr(NO<sub>3</sub>)<sub>2</sub> and 0.005 mol Na<sub>2</sub>CO<sub>3</sub> as starting materials in 50 ml ethylene glycol, without the use of any catalysts or calcination at high temperatures. The solutions were transferred into 125 ml flasks. Each was put in an ultrasonic bath (Bandelin SONOREX-RK 102 H, 120/480 W, 35 kHz, inner dimension: 22 cm long × 13.5 cm wide × 10 cm deep), and sonicated at 80 °C for 1 h, 3 h, and 5 h at a time. Calculated maximum intensity is 16,162 W m<sup>-2</sup>. The final products were washed with water and ethanol, and dried at 70 °C for 12 h.

The phases, vibration modes and morphologies of the products were characterized using X-ray diffraction (XRD)—recorded on a D-500 Siemens X-ray diffractometer with Cu Kα radiation and the diffraction angles of 2θ = 10–60° range, Bruker Tensor27 Fourier transform infrared (FTIR) spectrometer with KBr as a diluting agent—operated in 400–4000 cm<sup>-1</sup> range, transmission electron microscope (TEM)—carried out on a JEM-2010 JEOL TEM at 200 kV.

### 3. Results and discussion

Typical XRD patterns of the as synthesized SrCO<sub>3</sub> and BaCO<sub>3</sub> nanocrystallines are shown in Fig. 1. All diffraction peaks were identified to be orthorhombic SrCO<sub>3</sub>—compared to the JCPDS No. 05-0418 (*a* = 5.1070 Å, *b* = 8.4140 Å and *c* = 6.0290 Å and α = β = γ = 90°) and orthorhombic BaCO<sub>3</sub>—compared to the JCPDS No. 05-0378 (*a* = 5.3140 Å, *b* = 8.9040 Å and *c* = 6.4300 Å and α = β = γ = 90°)

\* Corresponding authors.

E-mail addresses: [ttthongtem@yahoo.com](mailto:ttthongtem@yahoo.com) (T. Thongtem),

[phuruangrat@hotmail.com](mailto:phuruangrat@hotmail.com) (A. Phuruangrat).

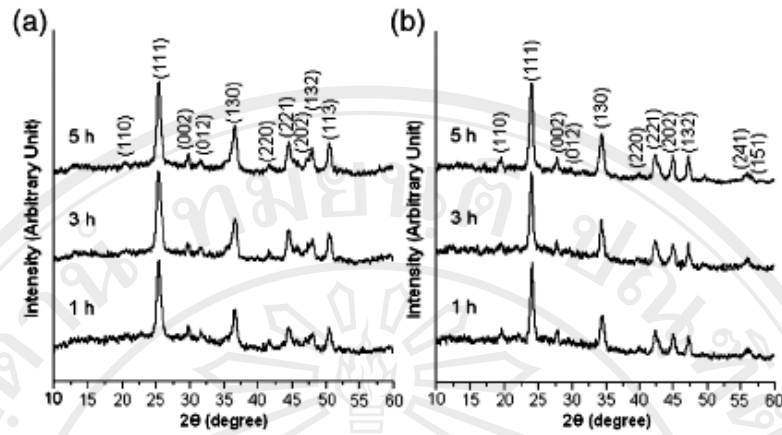


Fig. 1. XRD patterns of (a)  $\text{SrCO}_3$  and (b)  $\text{BaCO}_3$  synthesized by the sonochemical method at 80 °C for different lengths of times using  $\text{Sr}(\text{NO}_3)_2$  or  $\text{Ba}(\text{NO}_3)_2$  and  $\text{Na}_2\text{CO}_3$  as material sources.

[9]. Slightly broadened diffraction peaks with  $2\theta$  (°) of 20.45, 25.35, 29.73, 31.62, 36.58, 41.73, 44.52, 46.90, 48.02 and 50.43 were readily indexed as the (110), (111), (002), (012), (130), (220), (221), (202), (132) and (113) planes for  $\text{SrCO}_3$ ; and 19.54, 23.99, 27.68, 29.71, 34.32, 39.62, 42.42, 44.28, 44.98, 55.70 and 56.15 as the (110), (111), (002), (012), (130), (220), (221), (202), (132), (241) and (151) planes for  $\text{BaCO}_3$ , respectively. The increase in lattice parameters from  $\text{SrCO}_3$  to  $\text{BaCO}_3$  seems to relate with their ionic radii of these alkaline earth metals ( $\text{Sr}^{2+} = 0.125$  nm and  $\text{Ba}^{2+} = 0.142$  nm) [10].

The Scherrer formula [5] was used to determine the crystallite sizes of  $\text{SrCO}_3$  and  $\text{BaCO}_3$  as follows:

$$L = \frac{\lambda k}{B \cos \theta} \quad (1)$$

where  $\lambda$  is the wavelength of Cu K $\alpha$  radiation (0.154178 nm [1]),  $\theta$  is the Bragg angle at the (111) peaks of the XRD patterns,  $L$  is the average crystallite sizes of  $\text{SrCO}_3$  and  $\text{BaCO}_3$ ,  $k$  is the constant (0.89), and  $B$  is the full width at half maximum of the (111) peaks in radian. Calculated crystallite sizes of the products synthesized by the sonochemical method for 1 h, 3 h and 5 h are 8.74, 10.93 and

12.11 nm for  $\text{SrCO}_3$ , and 14.72, 16.38 and 19.52 nm for  $\text{BaCO}_3$ , respectively. These particle sizes were enlarged with the length of reaction time. At same length of time, the particle sizes of  $\text{BaCO}_3$  are larger than those of  $\text{SrCO}_3$ , due to the increase in their ionic radii and atomic masses.

Fig. 2 shows FTIR spectra of  $\text{SrCO}_3$  and  $\text{BaCO}_3$ , recorded in the 400–4000  $\text{cm}^{-1}$  wavenumbers. In general, the free planar  $\text{CO}_3^{2-}$  complexes have  $D_{3h}$  symmetry. The absorption bands were caused by the vibrations in  $\text{CO}_3^{2-}$  at 400–1800  $\text{cm}^{-1}$ . The strong absorption bands, centered at about 1449  $\text{cm}^{-1}$  for  $\text{SrCO}_3$  and 1447  $\text{cm}^{-1}$  for  $\text{BaCO}_3$ , are connected with the asymmetric stretching vibrations. Strong narrow absorption bands at about 865  $\text{cm}^{-1}$  and 707  $\text{cm}^{-1}$  for  $\text{SrCO}_3$ , and 862  $\text{cm}^{-1}$  and 696  $\text{cm}^{-1}$  for  $\text{BaCO}_3$  are assigned to be out of plane bending vibrations and in plane bending vibrations, respectively. Weak narrow absorption bands at about 1074  $\text{cm}^{-1}$  for  $\text{SrCO}_3$  and 1060  $\text{cm}^{-1}$  for  $\text{BaCO}_3$ , due to the symmetric stretching vibrations, were also detected [4–6,11]. It is worth to note that these vibrations were shifted from the higher wavenumbers for  $\text{SrCO}_3$  to the lower ones for  $\text{BaCO}_3$ , due to the covalent bonding of  $\text{M}^{2+}$  cations ( $\text{M} = \text{Sr}$  and  $\text{Ba}$ ) and  $\text{O}^{2-}$  anions in the  $[\text{CO}_3]^{2-}$  complexes—the cause of changing the efficient masses of the oscillating atomic

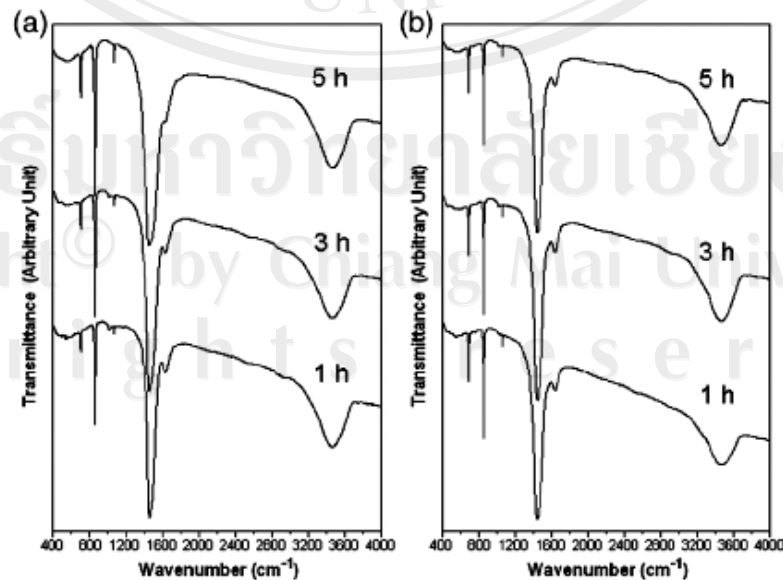


Fig. 2. FTIR spectra of (a)  $\text{SrCO}_3$  and (b)  $\text{BaCO}_3$  synthesized by the sonochemical method at 80 °C for different lengths of times.



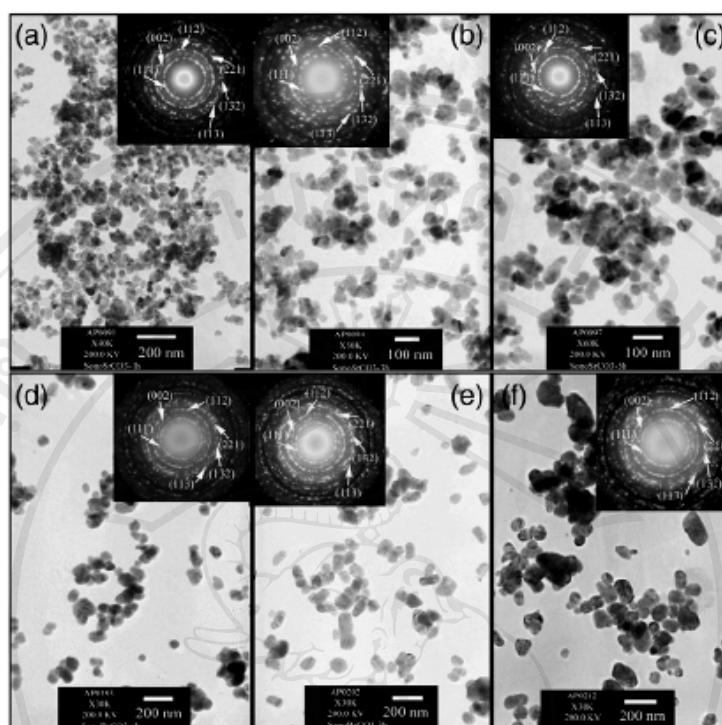


Fig. 3. TEM images and SAED patterns of (a–c)  $\text{SrCO}_3$  and (d–f)  $\text{BaCO}_3$  synthesized by sonochemical method at  $80^\circ\text{C}$  for 1 h, 3 h and 5 h, respectively.

groups. In addition, O–H stretching and bending vibrations of residual water were respectively detected at  $3466$  and  $1633\text{ cm}^{-1}$  for  $\text{SrCO}_3$ , and  $3462$  and  $1640\text{ cm}^{-1}$  for  $\text{BaCO}_3$ .

TEM images and SAED patterns of  $\text{SrCO}_3$  and  $\text{BaCO}_3$  are shown in Fig. 3. TEM shows that the products were composed of dispersed round nanoparticles with the sizes of  $20\text{--}50\text{ nm}$  for  $\text{SrCO}_3$  and  $40\text{--}100\text{ nm}$  for  $\text{BaCO}_3$ . Their SAED patterns appear as diffuse and hollow concentric rings of bright spots, caused by the diffraction of transmitted electrons through the nanocrystals with different orientations. Interplanar spaces were calculated using diameters of the diffraction rings [12], and compared with those of the JCPDS database [9]. They correspond to the (111), (002), (112), (221), (132) and (113) planes for both  $\text{SrCO}_3$  and  $\text{BaCO}_3$ . Their sizes were measured from 150 particles on TEM images. The products were synthesized in all sizes, ranging from the smallest to the largest with the average of  $29.83 \pm 4.26\text{ nm}$ ,  $34.02 \pm 5.26\text{ nm}$  and  $37.20 \pm 5.86\text{ nm}$  for  $\text{SrCO}_3$ , and  $55.20 \pm 9.60\text{ nm}$ ,  $65.00 \pm 10.04\text{ nm}$  and  $89.56 \pm 16.10\text{ nm}$  for  $\text{BaCO}_3$  by the 1 h, 3 h and 5 h ultrasonic irradiation, respectively.

To form  $\text{MCO}_3$  ( $\text{M}=\text{Sr}, \text{Ba}$ ) nanoparticles,  $\text{M}(\text{NO}_3)_2$  reacted with  $\text{Na}_2\text{CO}_3$  in ethylene glycol (EG) under ultrasonic irradiation (UIRR) by the reaction



Once the  $\text{MCO}_3$  nuclei formed in ethylene glycol by the assistance of ultrasonic irradiation, they did not fully develop. They grew into a number of nanoparticles via the diffusion process in EG. These nanoparticles became larger when the lengths of times were longer. They were still retaining their nanosize, although the reaction time was lengthened to 5 h. Comparing to the works of Alavi and Morsali [4,5],  $\text{Sr}(\text{CH}_3\text{COO})_2$  reacted with  $\text{NaOH}$  in ethanol with the aid of ultrasonic irradiation to form precursors ( $\text{Sr}(\text{OH})_2 \cdot \text{H}_2\text{O}$ ,  $\text{Sr}(\text{OH})_2 \cdot 8\text{H}_2\text{O}$  and  $\text{SrCO}_3$  mixtures), which were subsequently calcined at  $400^\circ\text{C}$  to

form  $\text{SrCO}_3$  [4]. When  $\text{Ba}(\text{CH}_3\text{COO})_2$  instead of  $\text{Sr}(\text{CH}_3\text{COO})_2$  was used,  $\text{BaCO}_3$  nanostructures were synthesized without the requirement of calcination [5].

#### 4. Conclusion

$\text{SrCO}_3$  and  $\text{BaCO}_3$  nanocrystallines were successfully synthesized by the ultrasonically irradiated method. The products are orthorhombic structures, specified by their XRD and SAED patterns. The vibration modes were studied using FTIR spectroscopy, and the morphologies including the particle sizes in nano-scale with good distribution using TEM.

#### Acknowledgement

This research was supported by the National Research University Project for Chiang Mai University, Commission on Higher Education, Ministry of Education, Thailand.

#### References

- [1] Li S, Zhang H, Xu J, Yang D. *Mater Lett* 2005;59:420–2.
- [2] Du J, Liu Z, Li Z, Han B, Huang Y, Zhang J. *Micropor Mesopor Mat* 2005;83:145–9.
- [3] Wang WS, Zhen L, Xu CY, Yang L, Shao WZ. *Crys Growth Des* 2008;8:1734–40.
- [4] Alavi MA, Morsali A. *Ultrason Sonochem* 2010;17:132–8.
- [5] Alavi MA, Morsali A. *Ultrason Sonochem* 2008;15:833–8.
- [6] Li L, Chu Y, Liu Y, Dong L, Huo L, Yang F. *Mater Lett* 2006;60:2138–42.
- [7] Gedanken A. *Ultrason Sonochem* 2004;11:47–55.
- [8] Mazloumi M, Zanganeh S, Kajbafvala A, Ghariniyat P, Taghavi S, Lak A, Mohajerani M, Sadrnezhad SK. *Ultrason Sonochem* 2009;16:11–4.
- [9] Powder Diffract. File, JCPDS-ICDD, 12 Campus Boulevard, Newtown Square, PA 19073–3273, U.S.A. 2001.
- [10] Phuruangrat A, Thongtem T, Thongtem S. *J Ceram Soc Japan* 2008;116:605–9.
- [11] Zhagn MX, Huo JC, Yu YS, Cui CP, Lei YL. *Chinese J. Struct Chem* 2008;27:1223–9.
- [12] Andrews KW, Dyson DJ, Keown SR. *Interpretation of electron diffraction patterns*. New York: Plenum Press; 1971.

## CURRICULUM VITAE

**Name** Mr. Narongrit Tipcompor

**Date of Birth** 13 June 1984

### Education Background

2007 - 2009 Master of Science (Inorganic Chemistry),  
Chiang Mai University

2003 - 2007 Bachelor of Science (Chemistry),  
Chiang Mai University

### Scholarship

2006 - 2009 The Center for Innovation in Chemistry: Postgraduate Education and  
Research Program in Chemistry (PERCH-CIC)

### Experiences

2007 - 2008 Undergraduate Teaching Assistant, Chiang Mai University,

- General Chemistry Laboratory
- Chemistry Laboratory for Health Science

ลิขสิทธิ์มหาวิทยาลัยเชียงใหม่  
Copyright © by Chiang Mai University

All rights reserved